The inositol-3-phosphate synthase biosynthetic enzyme has distinct catalytic and metabolic roles

Anna D. Frej[a], Jonathan Clark[b], Caroline Le Roy[c], Sergio Lilla[d], Peter Thomason[d], Grant P. Otto[a], Grant Churchill[5], Robert Insall[d], Sandrine P. Claus[c], Phillip Hawkins[b], Len Stephens[b] and Robin S.B. Williams[a#]

Centre for Biomedical Sciences, School of Biological Sciences, Royal Holloway University of London, Egham, Surrey, UK[a]; The Babraham Institute, Cambridge, Cambridgeshire, UK[b]; Department of Food and Nutritional Sciences, The University of Reading, Reading, Berkshire, UK[c]. CRUK Beatson Institute for Cancer Research, Glasgow, UK[4]. Department of Pharmacology, University of Oxford, Oxford, Oxfordshire, UK[5]

Running Head: Distinct catalytic and metabolic roles of Ino1

Address correspondence to Robin S.B. Williams, robin.williams@rhul.ac.uk.

Word count: Abstract 200

Material and Methods 7533

Intro/Results/Discussion/Legends 38183

ABSTRACT

Inositol levels, maintained by the biosynthetic enzyme inositol-3-phosphate synthase (Ino1), are altered in a range of disorders including bipolar disorder and Alzheimer's disease. To date, most inositol studies have focused on the molecular and cellular effects of inositol depletion without considering Ino1 levels. Here we employ a simple eukaryote, *Dictyostelium*, to demonstrate distinct effects of loss of Ino1 and inositol depletion. We show that loss of Ino1 results in inositol auxotrophy that can only be partially rescued by exogenous inositol. Removal of inositol supplementation from the *ino1*$^{-}$ mutant results in a rapid 56% reduction in inositol levels, triggering the induction of autophagy, reduced cytokinesis and substrate adhesion. Inositol depletion also caused a dramatic generalised decrease in phosphoinositide levels that was rescued by inositol supplementation. However, loss of Ino1 triggered broad metabolic changes consistent with the induction of a catabolic state that was not rescued by inositol supplementation. These data suggest a metabolic role for Ino1 independent of inositol biosynthesis. To characterise this role, an Ino1 binding partner containing SEL1L1 domains (Q54IX5) was identified with homology to mammalian macromolecular complex adaptor proteins. Our findings therefore identify a new role for Ino1, independent of inositol biosynthesis, with broad effects on cell metabolism.

INTRODUCTION

Myo-inositol, a stereoisomer of inositol, is present in a variety of cell types and is obtained from three major sources: *de novo* synthesis from glucose-6-phosphate, sequential dephosphorylation of phosphoinositides, or membrane transport from extracellular fluid (15). Disruption of inositol homeostasis has been associated with a number of illnesses, including bipolar disorder (3,4,61,74), Alzheimer's disease (2,41,68,72), bulimia (26), metabolic syndrome (39), diabetes

(30,52), and epilepsy (7). Understanding the cellular and metabolic changes resulting from inositol depletion will provide insight into the mechanisms underlying these diseases.

Inositol-3-phosphate synthase (Ino1, EC 5.5.1.4) is crucial in the *de novo* biosynthesis of inositol, as an isomerase that converts glucose-6-phosphate to inositol-3-phosphate, which is then dephosphorylated to inositol (33)(Fig 1A). Inositol is an essential precursor of a large family of phosphoinositides (14), with one of these, phosphoinositide 4,5 bisphosphate (PIP2), used in the production of inositol phosphates. These molecules are important for a range of cellular functions, including motility (42), activation of signal transduction pathways (18), membrane trafficking and vesicular transport (15), protein secretion, and transcriptional regulation (62). Despite these broad functions, few studies have compared the physiological effects of reducing inositol levels and reducing Ino1 levels, therefore it remains unclear if these two effects have distinct roles.

Dictyostelium discoideum is a single-celled eukaryote found in forest soils, where it survives by consuming bacteria. *Dictyostelium* is used as a research model in a variety of disciplines including biomedicine. We previously employed *Dictyostelium* in a 3Rs approach (animal reduction, replacement and refinement) for biomedical research, to investigate the effects of epilepsy treatments on modulating phosphoinositide signalling and seizure control (6,7) and the effects of bipolar disorder treatments on the level of inositol phosphates (19,74). These findings were successfully translated to mammalian disease models (7,19,60). *Dictyostelium* was also used to identify targets for compounds involved in bitter tastant detection (50,71) and conserved roles of homologues of human proteins (38,50), to investigate mitochondrial disease (25), Huntington's disease (73) and centrosomal organisation and function (29,66). These studies suggest that *Dictyostelium* can inform our understanding of cellular function relevant to human disease.

Dictyostelium has previously been employed to investigate the role of Ino1 in cell function (24), where insertional mutagenesis of *ino1* produced an inositol auxotrophic phenotype with a

concomitant decrease in inositol trisphosphate. Here, we independently deleted a key region of the *ino1* gene in an isogenic cell line, and find that growth of the *ino1*$^{-}$ mutant can only be partially rescued by exogenous inositol, suggesting a non-biosynthetic role for the protein. We further show that the previously described 'inositol-less death' is likely to lead to an upregulation of autophagy, loss of substrate adhesion and reduced cytokinesis resulting from inositol depletion. We also show that inositol depletion leads to a generalised reduction of phosphoinositide levels, without gross changes in metabolic profile. Surprisingly, we show that the greatest metabolic change is caused by loss of Ino1, and not by inositol depletion *per se*, since broad metabolic changes are not rescued by exogenous inositol, suggesting distinct effects of Ino1 loss and inositol depletion on cellular function. Finally, we identified a range of potential Ino1 binding partners, and confirmed direct Ino1 binding to a protein with mammalian homologues that serve as adaptors involved in the attachment to macromolecular complexes, providing a potential link to regulating inositol-independent cellular functions.

Materials and Methods

Materials - Axenic medium and LowFlo medium was purchased from ForMedium Co. Ltd (Hunstanton, UK). All restriction enzymes and First Strand cDNA synthesis kit were purchased from Fermentas (St Leon-Rot, Germany). Trizma hydrochloride (Tris-HCl), sodium chloride (NaCl), ethylenediaminetetraacetic acid (EDTA), 4′,6-diamidino-2-phenylindole (DAPI), cyclic adenosine monophosphate (cAMP), potassium phosphate monobasic (KH_2PO_4), potassium phosphate dibasic (K_2HPO_4), *myo*-inositol, and methanol were purchased from Sigma (Dorset, UK). The High Pure RNA isolation kit was purchased from Roche (Welwyn Garden City, UK). Penicillin-streptomycin and blasticidin were purchased from Life Technologies

(Gibco, UK). The DNasefree kit was purchased from Ambion (Austin, TX). The anti-RFP antibody was purchased from ChromoTek (Planegg-Martinsried, Germany).

Cell culture, strains and plasmids - All *Dictyostelium* axenic strains were grown at 22 °C in Axenic medium (Formedium Co. Ltd) containing 100 μg/ml penicillin and 100 μg/ml streptomycin. *Dictyostelium* transformants with a disrupted *ino1* gene were cultured in axenic medium with 10 μg/ml blasticidin and 500 μM *myo*-inositol.

Knock-out constructs were created by amplifying 5′ and 3′ fragments within the *ino1* gene by PCR from AX2 genomic DNA. The 5′ and 3′ PCR fragments were cloned into the pLPBLP expression vector (21), using BamHI-PstI and NcoI-KpnI restriction sites, respectively. The knock-out cassette was transformed into wild-type (AX2) cells and transformants were selected in axenic medium containing blasticidin (10 μg/ml). Independent clones of transformants resistant to blasticidin were screened for homologous integration by PCR. Loss of gene transcription was confirmed by reverse transcription PCR. For this purpose, RNA was extracted from the independent clones using the High Pure RNA isolation kit (Roche) according to the manufacturer's instructions. Contaminating DNA was removed using the DNasefree kit, followed by cDNA synthesis using the First Strand cDNA synthesis kit with 1 μg of RNA per sample. The cDNA was analysed by PCR to confirm loss of gene transcription (primers: GCTGCAAATCAAAAGGATCGTGCC and AAGGTGTTTTGTGGTGAACCATTGATG).

The Ino1-RFP overexpression construct was prepared using the full-length *ino1* (gene ID: DDB_G0285505) open reading frame. The gene was amplified from genomic DNA using EcoRI and BamHI as flanking restriction sites (primers: GAGCGAATTCATGTCAGCACAAATGTTTGAATC and TATGGATCCTAATCTTTGTTCTAATAACATG). The PCR products were cloned into an mRFPmars expression vector (389-2) under the control of the actin15 promoter (courtesy of

DrAnnette Müller-Taubenberger (1,23)). Constructs were transformed into the *ino1*$^{-}$ cell line by electroporation and selected for neomycin resistance (10 μg/ml). Expression of Ino1-RFP was confirmed by fluorescence microscopy and western blot analysis using anti-RFP antibodies. *ino1* gene expression was confirmed using reverse transcription PCR using the same method as described for generating an *ino1* knock-out cell line.

Development assays and cell image acquisition - Filter assays were used to develop *Dictyostelium* cells as described previously (74). Briefly, cells grown in the presence or absence (24 hours) of inositol (500 μM) were harvested in log-phase growth, and 1×10^7 cells/ml were plated on a 47 mm nitrocellulose filter (Millipore, Watford, UK). Filters were incubated for 24 hours at 22°C prior to imaging.

Substrate adhesion assay - *ino1*$^{-}$ or Ino1-RFP-expressing *ino*1^{-} cells grown in HL5 media in the presence of inositol (500 μM) were plated into 6-well plates, and the medium was replaced with HL5 media in the absence or presence of inositol (500 μM). After 24 hours the medium was gently removed with an aspirator to dispose of the non-adherent cells. Fresh medium was added and cells were immediately re-suspended and counted, and the processes was repeated for later timepoints.

Chemotaxis, Autophagy, and Cytokinesis assays - Chemotaxis assays were carried out using a Dunn chamber (Hawksley, Sussex, UK) as previously described (49). Images were recorded every 15 seconds over a 15 min period. Autophagy was measured in *ino1*$^{-}$ cells transformed with the *atg8-GFP* construct (Dictybase.org) (46). Cells were grown in Axenic medium with shaking for 72 hours (- inositol condition had inositol removed for 24 hours prior to the experiment), with 16 hour incubation in LoFlo medium (Formedium) to reduce the background autofluorescence. Cytokinesis defects were measured in cells cultured in shaking suspension for 72 hours, and inositol was removed where indicated 24 hours before the start of an assay, and cells were fixed

with 100% methanol at −20°C for 15 minutes, prior to labelling with 4′,6-diamidino-2-phenylindole (DAPI).

Immunoprecipitation - Initial co-immunoprecipitations were performed with the *ino1*$^{-}$ cell line constitutively expressing the *ino1-RFP* gene; *ino1*$^{-}$ cells constitutively expressing the *mRFPmars* gene on its own was used as a control (for 2 of 3 repeats) or wild-type (Ax2) cell lysate as a control. The presence of Ino1-RFP and RFP was confirmed by western blot analysis with anti-RFP antibodies. The gel was stained with Coomassie blue dye and the protein bands specific to Ino1-RFP (and absent in the RFP control) were evaluated by mass spectrometry and the data was analysed using Scaffold3 software.

The *ino1*$^{-}$ cell line co-transformed with *ino1-RFP* construct and *FLAG-gpmA*, *FLAG-pefB*, or *FLAG-Q54IX5* was used to perform a co-immunoprecipitation with anti-RFP coated beads to examine a direct interaction between Ino1 and these proteins. Ino1-GpmA and Ino1-Q54IX5 interactions were detected by western blot analysis with anti-RFP and anti-FLAG antibodies. The *ino1*$^{-}$ cell line co-transformed with the *ino1-RFP* construct and either *GFP-gpmA* or *GFP-Q54IX5* was used to perform co-immunoprecipitation with anti-GFP coated beads to confirm a direct interaction between Ino1 and these proteins; *ino1*$^{-}$ cells co-expressing *mRFPmars* and either *GFP-gpmA* or *GFP-Q54IX5* was used as a control for these experiments. The Ino1-Q54IX5 interaction was confirmed by western blot analysis with anti-GFP and anti-RFP antibodies.

Cells (3 x 10^8 per experiment) were washed with phosphate buffer, treated with 2.5 mM caffeine for 20 min with shaking, and lysed ((0.5% NP40, 40 mM Tris-HCl, 20 mM NaCl, 5 mM EGTA, 5 mM EDTA, 10 mM DTT, 1 mM PMSF, 2x protease and 2x phosphatase cocktail inhibitor (Roche – cat no. 11836170001 and 04906837001) on ice and the lysate was incubated with RFP-Trap or GFP-Trap agarose beads (ChromoTek GmbH) as per manufacturer's instructions. Briefly, the lysate was incubated with the beads for 1 hour at 4°C, then collected and washed twice (10

mM Tris-HCl, 150 mM NaCl, 0.5 mM EDTA, 1 mM PMSF, 2x protease and 2x phosphatase cocktail inhibitor (Roche)). The non-bound fraction was collected after this step. Immunocomplexes were dissociated from the beads by incubating at 70°C for 10 min in 4x TruPAGE LDS Sample Buffer (Sigma, PCG3009) and collected by centrifugation (the bound fraction) prior to the SDS-PAGE electrophoresis using either Sigma TruPAGE or BioRad pre-cast gel system. Protein presence was detected with anti-GFP [3H9] or anti-RFP [5F8] antibodies (ChromoTek GmbH), or a monoclonal anti-FLAG M2 antibody (Sigma, F3165), and recorded using the Odyssey Sa infrared imaging system.

NMR Spectrometry - Freeze-dried cell pellets were resuspended in 1 mL of Water/Methanol (1:2) and vortexed for polar metabolite extraction. Samples were then centrifuged at 2,400 g for 5 min and supernatants were kept for drying using a vacuum concentrator for 4.5 h at 45 °C. Once dried, samples were resuspended in 80 µL of phosphate buffer (in 90 % D_2O and 0.05 % sodium 3-(tri-methylsilyl) propionate-2,2,3,3-d4 (TSP) as a 1H NMR reference) and 50 µL of the solution was transferred into 1.7 mm capillary NMR tubes. Spectra were acquired at 300ºKon a Bruker Avance DRX 700 MHz NMR Spectrometer (Bruker Biopsin, Rheinstetten, Germany) operating at 700.19 MHz and equipped with a CryoProbe™ from the same manufacturer. All spectra were acquired using a 1-dimensional noesy pulse sequence [recycle delay – 90º - t1 – 90º - tm – 90º - acquire free induction decay (FID)] with water suppression applied during RD of 2 s, a mixing time (tm) of 100 ms and a 90º pulse set at 7.70 µs. For each spectrum, 512 scans were accumulated over a spectral width of 9803.9 Hz, and all FIDs were multiplied by a broadening line function of 0.3 Hz prior to Fourier transformation. All spectra were manually phased, baseline-corrected and calibrated to the TSP standard at δ 0.000 using the software MestReNova© (version 10.0.1, Mestrelab Research S.L., Spain).

Phospholipid Analysis - Glycerophospholipid levels were analysed by mass spectroscopy as previously described (9).

RESULTS

Ino1 protein is conserved from Dictyostelium to humans - To investigate the role of the *Dictyostelium* Ino1 protein, we first compared the *Dictyostelium* (Q54N49) and human (Q9NPH2-1) protein sequences (Fig 1B,C). The proteins share 59% sequence identity throughout their length, are of similar size and show common conserved NAD-binding and catalytic domains (Fig 1B) that are present in Ino1 proteins from species across distant biological kingdoms (Fig 1C), suggesting a highly conserved catalytic role of Ino1 throughout evolution and supporting the use of *Dictyostelium* to analyze Ino1 function.

ino1$^-$ *is an inositol auxotroph* - To analyse the effect of Ino1 loss and inositol depletion on *Dictyostelium* cell growth and development, we ablated 19% of the *ino1* coding sequence, including two regions encoding highly conserved amino acid motifs, by homologous integration of a knockout cassette (Fig 1B-F). The resultant *ino1*$^-$ cells were unable to grow in liquid medium without inositol supplementation above 50 µM (Fig 2A), consistent with that shown previously (24). However, unlike this previous study, inositol supplementation did not fully restore the *ino1*$^-$ growth rate to that of the wild-type, reaching a maximal level of growth at 300 µM with higher concentrations not increasing growth.

In *Dictyostelium*, starvation triggers cell differentiation and morphogenesis to form spore-bearing fruiting bodies. We thus investigated the effect of Ino1 loss, with and without inositol supplementation, on multicellular development. Wild-type and *ino1*$^-$ cells were starved on nitrocellulose filters for 24 hours, and fruiting body morphology was recorded (Fig 2B). *ino1*$^-$ cells grown in the absence of inositol for 24 hours prior to nutrient deprivation were able to aggregate but formed aberrant fruiting bodies (Fig 2B), a phenotype not observed for *ino1*$^-$ cells in an earlier report (24); however, inositol supplementation (500 µM) prior to the assay enabled *ino1*$^-$ cells to produce mature fruiting bodies with wild-type morphology.

Both growth and development phenotypes were due to lack of the Ino1 protein. This was shown by expression of Ino1 linked to a C-terminal red fluorescent protein (RFP) tag in *ino1*$^-$ cells, which restored wild-type growth and development with the resulting functional protein showing a cytosolic localisation (Fig 2 D,E,F,G). Interestingly, since exogenous inositol did not fully restore the wild-type growth rate in *ino1*$^-$ cells, it is likely that cells require the Ino1 protein for normal growth. *ino1*$^-$ cells were also unable to grow on a bacterial lawn (Fig 2G), as reported previously (29), even with inositol supplementation. These results confirm a vital role of inositol in *Dictyostelium* growth and development, consistent with that shown in a variety of organisms throughout the kingdoms of life (40).

Ino1 loss triggers inositol depletion - Our data show that a block in cell growth and altered development results from the removal of exogenous inositol in the *ino1*$^-$ mutant, and thus we quantified inositol levels by NMR in the *ino1*$^-$ and wild-type cells in the presence or absence of added inositol (Fig 3A). Wild-type cells grown in un-supplemented medium contained 1.5 ± 0.1 µM inositol, and this significantly increased to 3.4 ± 0.1 µM following inositol supplementation ($p < 0.0001$), and returned to baseline following removal of inositol (Fig 3A). In contrast, *ino1*$^-$ cells grown with inositol supplementation had an intermediate level of inositol (1.8 ± 0.1 µM) that significantly decreased to 0.8 ± 0.1 µM following removal of exogenous inositol for 12 hours ($p = 0.0013$). A reduced level was maintained following 24 hour starvation (1.2 ± 0.1 µM), and returned to 2.0 ± 0.1 µM following re-introduction of inositol (Fig 3B). These data confirm that in *ino1*$^-$ cells, inositol was depleted following withdrawal of exogenous inositol, and this trend is consistent with that reported earlier (24). In addition, this data suggests that the *ino1*$^-$ mutant supplemented with inositol has similar intracellular inositol levels to wild-type cells (without supplementation), and that differences between these cell types are likely to arise from an absence of the enzyme, enabling a range of experiments to provide new insights into the distinct cell and metabolic changes caused by inositol depletion and loss of Ino1.

Ino1 loss causes a pleiotropic phenotype - We first investigated potential changes in cell movement during chemotaxis toward cAMP (Fig 3B). In these experiments, wild-type cells showed a velocity of 9.63 ± 1.49 μm/min, with an elongated shape (aspect), and tendency for single directional movement (directness) of 0.87 ± 0.14. Loss of Ino1, without inositol depletion, caused a significant loss of elongated shape, suggesting an Ino1-dependent change. In contrast, inositol depletion in *ino1*$^-$ cells significantly reduced cell speed, whilst the loss of shape that was also observed for Ino1 deletion was retained, and showed increased persistence. These data suggest distinct effects specific to Ino1 loss (related to loss of cell shape) and to inositol depletion (loss of velocity).

We then examined the mechanism leading to the block in cell growth caused by loss of Ino1 in the absence of exogenous inositol, previously termed '"inositol-less death" (56). Since autophagy can lead to cell death in response to cell stress or nutrient depletion (34), we tested whether inositol depletion triggered an autophagic response. In *Dictyostelium*, formation of autophagosomes can be visualised by the incorporation of a fluorescently-tagged autophagy-related protein 8 (Atg8) into autophagosomal membranes (46). The *ino1*$^-$ strain, grown in the absence of inositol for 24 hours (but without nutrient depletion), showed a four–fold increase in autophagosome number per cell compared to the wild-type strain (Fig 3C,D). These data suggest that inositol depletion triggered an autophagic response in *ino1*$^-$ cells.

We also examined the effect of Ino1 loss and inositol depletion on substrate attachment and cytokinesis. To assess changes in cell adhesion, the number of cells attached to plates was quantified up to 72 hours following the removal of exogenous inositol from the *ino1*$^-$ mutant. In the presence of inositol (500 μM), *ino1*$^-$ cells proliferated up to 24 hours and remained adherent (Fig 3E). Upon removal of exogenous inositol, *ino1*$^-$ cell number decreased to 88.5% of inositol-supplemented cells after 24 hours, and to 33.5% after 72 hours. *ino1*$^-$ cells expressing *ino1-RFP* did not lose adhesion in the absence of exogenous inositol. Secondly, we assessed cytokinesis by

comparing the number of nuclei per cell in the *ino1*$^{-}$ and wild-type strains, in the presence of inositol or following inositol depletion, using DAPI nuclear stain (Fig 3F,G) (47). In these experiments, *ino1*$^{-}$ cells showed a significant ($p < 0.001$) increase in nuclei number following inositol depletion compared to the wild-type strain. Under inositol depletion conditions, 24.7% of the *ino1*$^{-}$ cells accumulated ≥ 3 nuclei compared to 7.7% of the wild-type cells. This effect was rescued by growing *ino1*$^{-}$ cells in the presence of inositol (500 μM) (9.7% of cells accumulated ≥ 3 nuclei) or by overexpressing *ino1*-RFP (Fig 3F,G) (10% of cells accumulated ≥ 3 nuclei). These data suggest that inositol depletion leads to an increase in autophagy, a loss of cell-substrate adhesion and a reduction in cytokinesis, but loss of Ino1 *per se* did not trigger these responses.

Inositol depletion regulates phospholipid levels - Since inositol is a precursor to a family of inositol phospholipids (Fig 4A, B), we examined changes in phospholipid levels due to both the loss of Ino1 and as a result of inositol depletion. In *Dictyostelium*, two types of phospholipids are present, diacyl phospholipids containing two acyl linkages to the glycerol backbone, and the recently reported ether/acyl phospholipids containing a glycerol backbone linked to a fatty alcohol at position 1 (9) (Fig 4A). We quantified the levels of both phospholipid species in wild-type and *ino1*$^{-}$ cells grown in the presence and absence of inositol (Fig 4C-Q). Separation of distinct phospholipid species was limited to those of different molecular weights. We first examined levels of the phospholipid precursor phosphatidic acid (PA), which comprises a glycerol backbone and two fatty acid tails. Both diacyl-linked and ether-linked PA levels decreased during early inositol depletion in *ino1*$^{-}$ cells (Fig 4C,D). Phosphatidylinositol (PI), which is formed by the addition of the inositol head group to PA, decreased following inositol depletion (in *ino1*$^{-}$), with the greatest reduction seen in diacyl-linked PI (Fig 4E,F,). A similar effect was seen for the diacyl phosphatidylinositol monophosphate (PIP) (Fig 4G,H). Surprisingly, inositol depletion induced a reduction in diacyl phosphatidylinositol bisphosphate (PIP2) but not in ether/acyl PIP2 (Fig 4I,J). For phosphatidylinositol trisphosphate (PIP3), only

ether/acyl PIP3 was detectable in *ino1*$^{-}$ cells, and was reduced compared to wild-type cells, independent of exogenous inositol supply (Fig 4K). The reintroduction of inositol for 12 hours after 24 hour starvation restored the levels of the majority of ether/acyl and diacyl phospholipids. These data suggest that the pool of diacyl phospholipids is more sensitive to inositol depletion than ether/acyl species, and that cellular ether/acyl PIP2 levels are maintained during these conditions.

Since a reduction in inositol synthesis attenuates the production of phosphoinositides, and causes a transient reduction of PA, we then monitored changes in other phospholipids during inositol depletion and rescue. No change in phosphatidylserine (PS) was seen in wild-type cells under any condition tested; however, *ino1*$^{-}$ cells depleted of inositol for 24 hours showed a non-significant increase in PS that was further elevated following inositol replenishment for both ether/acyl and diacyl species (Fig 4L,M). Other phospholipids, containing ethanolamine and choline head groups, did not change in wild-type or *ino1*$^{-}$ cells under any condition (Fig 4N-Q).

Ino1 loss causes a shift to catabolic metabolism - We next investigated the metabolic consequences of both the loss of Ino1 and inositol depletion using wild-type and *ino1*$^{-}$ cells grown in the presence and absence of inositol (Fig 5). Both ablation of *ino1* and inositol treatment induced specific metabolic changes. Principal component (PC) analysis of metabolic profiles suggested that the greatest metabolic change was observed between the wild-type and *ino1*$^{-}$ cells independent of exogenous inositol provision (Fig 5A,B), where *ino1* ablation accounted for 53% of the total variance as observed in PC1. The mutation resulted in an increase in amino acids and compounds related to amino acid breakdown (alanine, aspartate, isoleucine, lysine, methionine, GABA, putrescine), in energy-related metabolites (fumarate, lactate), in adenosine phosphorylated derivatives (5'-AMP, 3'-AMP, ATP, cAMP) and in sn-glycero-3-phosphocholine (GPC), a potent osmolyte (Fig 5B). In contrast, inositol treatment accounted for only 12% of the variance between the metabolic profiles of wild-type and *ino1*$^{-}$ cells as observed in PC2 (Fig

315 5A,C). In *ino1*$^{-}$ cells, inositol treatment resulted in increased amino acid levels (leucine,
316 methionine, tyrosine). These data suggest a dominant role for the presence of the Ino1 protein
317 (rather than inositol levels) in metabolic regulation (Fig 5).

318 Ino1 absence caused a major shift in metabolic profile, and we therefore specifically examined
319 changes caused by Ino1 loss (Fig 6A,B). This analysis showed changes in many of the metabolic
320 products found in the initial PC analysis. In contrast to a loss of Ino1, inositol depletion caused
321 limited changes to metabolic profiles. Here we specifically compared *ino1*$^{-}$ cells grown in the
322 presence or absence of inositol (12 and 24h treatments were combined since they resulted in
323 similar metabolic changes and inositol levels) (Fig 6C,D) to show that inositol supplementation
324 led to an increase of inositol and lipids, consistent with the phosphoinositide analysis (Fig 4).
325 Interestingly, reintroduction of inositol for 12 hours after 24 hour inositol depletion changed the
326 metabolic profile of *ino1*$^{-}$ cells (Fig 6E,F).

327 Supervised analysis was then used to specifically evaluate the impact of Ino1 loss on cell
328 metabolism (Fig 7). This approach suggested that Ino1 loss was associated with a significant
329 increase in some amino acids (alanine, aspartate, glycine, GABA, isoleucine, lysine, methionine),
330 and in metabolites associated with regulation of the cell cycle and DNA metabolism (guanosine,
331 ATP, deoxy-ADP, 5'AMP, 3'AMP, UTP, and β-alanine, a biomarker of the degradation of
332 pyrimidines (17)). Putrescine was also significantly increased, consistent with a reduction in cell
333 proliferation, as previously demonstrated in *Dictyostelium* (35). An increase in lactate was also
334 observed, which suggests an increase in the $NADH+H^{+}/NAD^{+}$ ratio that stimulates the activity
335 of the lactate dehydrogenase. An increase in $NADH+H^{+}/NAD^{+}$ ratio would simultaneously
336 inhibit the citrate synthase and slow down the Krebs cycle, resulting in an accumulation of some
337 intermediates. This is consistent with the accumulation of acetate, derived from the spontaneous
338 hydrolysis of oxaloacetate, and of fumarate and succinate, two other intermediates of the Krebs

cycle. Finally, sn-glycero-3-phosphocholine (GPC) was greatly increased, suggesting that the lack of Ino1 was compensated by the production of a strong osmolyte. The increased $NADH+H^+/NAD^+$ ratio is a signature of catabolic reactions. Together, these data suggest that the loss of Ino1 shifts cells into a catabolic state. Together with the observation of markers of reduced cell proliferation, these data further support the autophagic phenotype of *ino1*$^-$ mutants, even when supplemented with inositol.

Supervised analysis was also used to evaluate the impact of inositol depletion on individual metabolites (Fig 7). This approach suggested that inositol depletion resulted in changes in some amino acids (increases in alanine, GABA, glycine, and valine, and a decrease in phenylalanine), an increase in lactate, fumarate, and succinate, and a decrease in 3'AMP, guanosine, and glycogen. No effect on the metabolic profile was shown due to the selection antibiotic (blasticidin) for the *ino1*$^-$ cells (O-PLS model parameters: $R^2Y = 0.18$ and $Q^2Y = 0$). Although we observed that the mutants were already in a catabolic state, the addition of inositol tended to moderate this metabolic phenotype, since indicators of anabolism (glycogen and lipids) were higher in cells supplemented with inositol, while those not supplemented were associated with markers of catabolism (i.e. lactate and succinate). Thus, these results suggest that the absence of Ino1, rather than inositol depletion, triggered broad metabolic changes.

Mutation of an Ino1 catalytic residue reduces growth, independent of exogenous inositol - To investigate a role for Ino1 that is independent of catalytic activity, we expressed a mutated Ino1 lacking a key catalytic aspartic acid (D342A) that is conserved throughout the tree of life (40). Wild-type cells expressing this construct showed strongly reduced growth, either in the presence or absence of inositol (500 µM; Fig 8A), suggesting a dominant negative effect of the protein. *ino1*$^-$ cells expressing this construct retained the inositol auxotrophic phenotype, confirming a lack of catalytic activity of the mutated protein, but additionally showed strongly reduced growth in the presence of inositol (500 µM).

Ino1 binds a possible macromolecular complex linker protein - To investigate a mechanism for Ino1 in regulating cell function independent of catalytic activity, Ino1 binding partners were isolated by co-immunoprecipitation. Ino1-RFP was expressed in *ino1*$^{-}$ cells, bound to agarose beads coated with anti-RFP antibody, and Ino1 binding proteins were purified by co-immunoprecipitation, followed by separation by SDS-PAGE and identification by mass spectrometry (Fig 8B). This approach identified 104 potential binding partners from three independent experiments. Potential binding partners were divided into six major groups: actin-related, immunity and stress, metabolism, nucleic acid related (translation, transcription, regulation of gene expression and DNA recombination), protein catabolism, modification and transport, and others encompassing signal transduction, ATP hydrolysis and proton transport (including V-type proton ATPase catalytic subunits A and B) (Supplementary data). We extended our analysis for three potential Ino1 binding proteins: GpmA, a phosphoglycerate mutase protein; PefB, a penta-EF hand domain-containing protein; and Q54IX5, an uncharacterised protein with three Sel1-like repeats (Fig 8C,D). These proteins tagged with a FLAG epitope were co-expressed in cells with Ino1-RFP, and Ino1-RFP was immunoprecipitated from cell lysates with RFP antibody linked to agarose beads. The bound protein fractions were then analysed for the presence of each FLAG-tagged protein, demonstrating that GpmA-FLAG bound weakly, whereas Q54IX5-FLAG bound strongly to Ino1-RFP (Fig 8C). The Q541X5-Ino1 interaction was confirmed using the reverse approach, where Q54IX5-GFP was coexpressed with Ino1-RFP, and immunoprecipitated with a GFP antibody linked to agarose beads; co-immunoprecipitated Ino1-RFP was detected by Western blot with an RFP antibody (Fig 8D). These approaches confirmed that Q54IX5 binds strongly to Ino1.

DISCUSSION

Inositol and inositol-containing compounds are vital cellular components, and a range of studies have identified pleiotropic effects of inositol depletion on cell function, but have not considered

complications due to altered levels of the biosynthetic enzyme, Ino1. To distinguish between the effects of inositol depletion and a loss of Ino1 on cell function and metabolism, we ablated the inositol biosynthetic enzyme, Ino1, in *Dictyostelium*, and compared wild-type cells and cells without Ino1 in the presence and absence of inositol. Loss of Ino1 produced an inositol auxotroph phenotype during growth and blocked development, confirming an earlier *Dictyostelium* study (24), and results from diverse organisms ranging from *Saccharomyces cerevisiae* (13) to mice (45), demonstrating the essential conserved role of inositol in cellular function. We show that the *myo*-inositol levels decreased in the *ino1*$^{-}$ mutant by 36-56% (depending upon starvation time), and return to pre-depletion levels following inositol replenishment. This inositol depletion response is consistent with an obligate role for inositol production catalysed by Ino1. We show that inositol depletion resulting from *ino*1 ablation blocks development, reduces cell velocity, upregulates autophagy, and inhibits cytokinesis, consistent with a range of studies in other systems (12, 24, 37, 51, 62), and confirming the validity of this model to study Ino1 function. All of these phenotypes, except growth and cell shape, are rescued by provision of exogenous inositol, and are thus likely to be due to inositol depletion rather than loss of Ino1.

Dysregulation of inositol levels has been reported in a wide range of biomedical and clinical studies, relating to both disease conditions and as a result of medicinal treatment, although few studies have addressed specific changes in Ino1 protein levels. A range of structurally independent bipolar disorder drugs, including carbamazepine, valproate and lithium, act via an inositol depletion mechanism (74), and induce autophagy *in vitro* and *in vivo* (43,67), most likely as a mechanism to promote survival by recycling cellular components (12,51). Altered inositol levels have also been demonstrated in patient studies of bipolar disorder (58), major depressive disorder (10), and schizophrenia (59). For these reasons, modulating inositol levels was proposed as a therapy in the treatment of bipolar disorder (8), depression, and panic disorders (48). In addition, Ino1 activity and protein levels are elevated in post-mortem brains of Alzheimer's

patients (57), although studies showed pathologically-lowered inositol levels and mitochondrial dysfunction in mouse models of Alzheimer's disease (68) that could be linked to autophagy (36). However, no distinction has been made in these studies between altered inositol levels and altered Ino1 levels. In our present study, we have separated the effects caused by altered Ino1 levels and inositol depletion, to provide a unique approach to monitor cellular and metabolic changes relating to inositol levels.

Since phosphoinositide production is the first step of inositol incorporation into cell signalling, we examined the effect of loss of Ino1 and inositol depletion and replenishment on this family of chemicals, analysing both diacyl-linked and ether/acyl-linked compounds independently (9). Inositol depletion induced a rapid reduction in both species of PI and PIP, and strongly reduced diacyl PIP2 levels, but had little effect on ether/acyl PIP2. Surprisingly, PIP3 was greatly reduced in the *ino1*$^{-}$ mutant, under all conditions, independent of exogenous inositol. Overall, the greater reduction in diacyl-phosphoinositides may be due to these phospholipids comprising under 5% of the inositol phospholipids (9), leading to rapid metabolism. Alternatively, these compounds may provide a more labile signalling component compared to ether-derived compounds, and further research could investigate these alternatives. Nevertheless, this data shows a critical effect of inositol depletion in regulating phosphoinositides.

These results also support studies demonstrating an important role for diacyl PIP2 in vesicle formation and transport (32) and in membrane trafficking at the neuronal synapse (11). In *Dictyostelium,* ablation of a PIP2 biosynthetic enzyme PIP5 kinase (PikI) led to a 90% reduction in PIP2 levels, and disorientated cell movement (22). The pivotal role of PIP2 in these processes suggests a requirement for cells to maintain the levels of this essential molecule during inositol starvation. Cytokinesis, the final part of the cell division process, is also critically dependent upon an increase in PIP2 levels (37). Our analysis shows a 65% reduction in diacyl PIP2 levels following 24-hour inositol depletion, and is consistent with this phospholipid playing a critical

role in cytokinesis, as evidenced by the multinucleate phenotype of *ino1*$^{-}$ cells. In a similar manner, PIP2 is involved in substrate attachment by regulating actin polymerisation and depolymerisation (37) that may result in a reduced cell-substrate adhesion. Overall, the data suggest that inositol depletion has a fundamental and rapid effect on phosphoinositide regulation that is likely to result in wide-ranging changes in cellular function and cell health.

Interestingly, Ino1 may play a role in regulating PIP3 levels regardless of inositol level, since the *ino1*$^{-}$ mutant grown in inositol-supplemented medium showed reduced PIP3 levels, even though intracellular *myo*-inositol levels were comparable to those of wild-type cells. Previous studies in *Dictyostelium* demonstrated that a complete block in PIP3 production, by deletion of all five type-1 phosphoinositide 3-kinase enzymes, resulted in poor growth in suspension and developmental defects (27). Combined, these findings suggest that loss of the Ino1 protein leads to a loss of PIP3 production, resulting in poor cell growth.

We also examined metabolic changes caused by loss of the Ino1 protein and during inositol depletion. Surprisingly, the greatest metabolic change observed here was due to an absence of Ino1, independent of the inositol level, which gave rise to elevated amino acids, energy-related components, DNA regulation and osmolytes. This metabolic shift was not due to altered inositol levels *per se*, since cellular inositol levels are consistent between the mutant and wild-type cells during inositol supplementation, but rather an absence of the Ino1 protein. These changes are likely to have a major effect on cellular function, and suggest an important non-catalytic role for the protein in metabolic regulation. We thus propose a key role for Ino1 in regulating metabolism through an inositol homeostasis-independent mechanism, and that *ino1* ablation induces a shift in metabolism towards an autophagic response, consistent with increased levels of putrescine, amino acids and nucleotide derivatives (31). In contrast, inositol depletion caused general changes in lipids, and from the wide range of specific compounds assessed, variable changes in a few

amino acids were found. This suggests inositol depletion has little metabolic effect in the short timescale examined in this study.

Since inositol supplementation did not fully restore *ino1*$^{-}$ growth, we expressed a mutant protein Ino1-D342A in these cells and assessed growth. This mutation is likely to disrupt catalytic activity and is conserved in all known Ino1 proteins. Expression of Ino1-D342A did not rescue the inositol auxotrophy resulting from Ino1 loss, and thus does not catalyse inositol biosynthesis. In contrast, expression of the protein reduced growth in all strains, independently of exogenous inositol provision. Further studies will be necessary to determine if this response is due to the depletion of the Ino1 substrate, inactivation of a potential Ino1 multimeric complex, or by other mechanisms.

To identifying new roles for Ino1 in regulation of cellular function, we isolated a number of potential Ino1 binding partners. These included proteins related to cytoskeletal organisation, mitochondrial respiration chain, proton transport, DNA and protein regulation, and metabolism, including fatty acid, glycolysis and purine metabolism; these potential interactors are consistent with those identified in *S. cerevisiae* (63,64) and in humans (20). In addition, components of the peripheral V1 complex of the vacuolar ATPase were identified, which are responsible for acidifying intracellular compartments in eukaryotic cells, and these have also been identified as Ino1 interactors in *S. cerevisiae* (16). From the list of potential binding partners, we independently confirmed Ino1-GpmA binding, where GpmA is involved in the interconversion of 2- and 3-phosphoglycerate, and 2,3-bisphosphoglycerate (2,3 BPG) is a potent inhibitor of $InsP_3$ 5'-phosphatase and also $InsP_2$ dephosphoryation (70) and is elevated following *ino1* loss in *Dictyostelium* (24). We also confirmed strong Ino1-Q54IX5 binding, where this protein contains a tetratricopeptide repeat (TPR) that mediates protein-protein interactions, often during the assembly of multiprotein complexes (5). Although the function of an Ino1-Q54IX5 interaction remains to be examined, the potential human orthologue of Q54IX5 is the SEL1L protein that is

involved in the movement of misfolded proteins from the ER to the cytosol (44), and thus deregulation of this protein in the *ino1*$^{-}$ mutant may have far-reaching effect on cell metabolism.

Since we show that the absence of Ino1 and inositol depletion have different molecular and metabolic effects, we question whether these effects are interrelated. Inositol depletion has been shown to activate *ino1* expression in a wide range of models (55,69), including *Dictyostelium* (74), and mice (54); this effect is likely to elevate Ino1 levels. Many studies have relied on using inositol depleting drugs prescribed as bipolar disorder treatments, which act through multiple targets (28,53,65,75), and hence these results are likely to be complicated by secondary effects. In contrast, our studies did not utilise drug treatments, and our results suggest that short-term inositol depletion does not cause large metabolic changes in *Dictyostelium*, with a resulting increase in *ino1* transcription acting to reverse this deficit (74). This responsive regulation would protect cells against a transient reduction in inositol levels without triggering large metabolic changes. However, a dysregulation of this responsive mode, resulting from a reduction of Ino1 levels, is likely to cause wide-ranging metabolic effects, independent of inositol provision.

Our studies show that a loss of the crucial inositol biosynthetic enzyme Ino1 and inositol depletion cause discrete cellular, molecular and metabolic effects. Although inositol depletion alters cell physiology, triggering an autophagic response, loss of substrate adhesion, reduction in cell division, and a rapid reduction in a range of phospholipids, it does not trigger a large change in metabolic profile. In contrast, the Ino1 protein itself plays an important role in cell growth and shape and metabolic regulation, regardless of inositol level, including the binding to a linker protein, Q54IX5, suggesting further roles of this protein.

Acknowledgments

None

Funding information

This work was funded by a grant to RSBW by The Dr Hadwen Trust for Humane Research (DHT), which is the UK leading medical research charity that funds and promotes exclusively human-relevant research that encourages the progress of medicine with the replacement of the use of animals in research. GO was supported by NC3Rs Grant NC/M001504/1.

Conflict of interests

None.

Author Contributions

RSBW and AF planned the experiments. AF, JC, CLR, GPO, GC, SPC, PH, LS, SL, PT, RI carried out all experimental procedures and data analysis. RSBW and AF wrote the paper.

Supplementary data will be available at the following site: DOIxxxxx

Reference List

1. **Basu, S., P. Fey, Y. Pandit, R. Dodson, W. A. Kibbe, and R. L. Chisholm**. 2013. DictyBase 2013: integrating multiple Dictyostelid species. Nucleic Acids Res. **41**:D676-D683. doi:gks1064 [pii];10.1093/nar/gks1064 [doi].

2. **Berridge, M. J.** 2014. Calcium regulation of neural rhythms, memory and Alzheimer's disease. J.Physiol **592**:281-293. doi:jphysiol.2013.257527 [pii];10.1113/jphysiol.2013.257527 [doi].

3. **Berridge, M. J.** 2014. Calcium signalling and psychiatric disease: bipolar disorder and schizophrenia. Cell Tissue Res. **357**:477-492. doi:10.1007/s00441-014-1806-z [doi].

4. **Berridge, M. J., C. P. Downes, and M. R. Hanley**. 1989. Neural and developmental actions of lithium: a unifying hypothesis. Cell **59**:411-419.

5. **Blatch, G. L. and M. Lassle**. 1999. The tetratricopeptide repeat: a structural motif mediating protein-protein interactions. Bioessays **21**:932-939. doi:10.1002/(SICI)1521-1878(199911)21:11<932::AID-BIES5>3.0.CO;2-N.

6. **Chang, P., B. Orabi, R. M. Deranieh, M. Dham, O. Hoeller, J. A. Shimshoni, B. Yagen, M. Bialer, M. L. Greenberg, M. C. Walker, and R. S. Williams**. 2012. The antiepileptic drug valproic acid and other medium-chain fatty acids acutely reduce phosphoinositide levels

independently of inositol in Dictyostelium. Dis.Model.Mech. **5**:115-124. doi:dmm.008029 [pii];10.1242/dmm.008029 [doi].

7. **Chang, P., M. C. Walker, and R. S. Williams**. 2014. Seizure-induced reduction in PIP3 levels contributes to seizure-activity and is rescued by valproic acid. Neurobiol.Dis. **62**:296-306. doi:S0969-9961(13)00292-1 [pii];10.1016/j.nbd.2013.10.017 [doi].

8. **Chengappa, K. N., J. Levine, S. Gershon, A. G. Mallinger, A. Hardan, A. Vagnucci, B. Pollock, J. Luther, J. Buttenfield, S. Verfaille, and D. J. Kupfer**. 2000. Inositol as an add-on treatment for bipolar depression. Bipolar.Disord. **2**:47-55.

9. **Clark, J., R. R. Kay, A. Kielkowska, I. Niewczas, L. Fets, D. Oxley, L. R. Stephens, and P. T. Hawkins**. 2014. Dictyostelium uses ether-linked inositol phospholipids for intracellular signalling. EMBO J. **33**:2188-2200. doi:embj.201488677 [pii];10.15252/embj.201488677 [doi].

10. **Coupland, N. J., C. J. Ogilvie, K. M. Hegadoren, P. Seres, C. C. Hanstock, and P. S. Allen**. 2005. Decreased prefrontal Myo-inositol in major depressive disorder. Biol.Psychiatry **57**:1526-1534. doi:S0006-3223(05)00233-7 [pii];10.1016/j.biopsych.2005.02.027 [doi].

11. **Cremona, O. and C. P. De**. 2001. Phosphoinositides in membrane traffic at the synapse. J.Cell Sci. **114**:1041-1052.

12. **Criollo, A., M. C. Maiuri, E. Tasdemir, I. Vitale, A. A. Fiebig, D. Andrews, J. Molgo, J. Diaz, S. Lavandero, F. Harper, G. Pierron, S. D. di, R. Rizzuto, G. Szabadkai, and G. Kroemer**. 2007. Regulation of autophagy by the inositol trisphosphate receptor. Cell Death.Differ. **14**:1029-1039. doi:4402099 [pii];10.1038/sj.cdd.4402099 [doi].

13. **Culbertson, M. R., T. F. Donahue, and S. A. Henry**. 1976. Control of inositol biosynthesis in Saccharomyces cerevisiae: properties of a repressible enzyme system in extracts of wild-type (Ino+) cells. J.Bacteriol. **126**:232-242.

14. **De Camilli, P., S. D. Emr, P. S. McPherson, and P. Novick**. 1996. Phosphoinositides as regulators in membrane traffic. Science **271**:1533-1539.

15. **Deranieh, R. M. and M. L. Greenberg**. 2009. Cellular consequences of inositol depletion. Biochem.Soc.Trans. **37**:1099-1103. doi:BST0371099 [pii];10.1042/BST0371099 [doi].

16. **Deranieh, R. M., Y. Shi, M. Tarsio, Y. Chen, J. M. McCaffery, P. M. Kane, and M. L. Greenberg**. 2015. Perturbation of the Vacuolar ATPase: A NOVEL CONSEQUENCE OF INOSITOL DEPLETION. J.Biol.Chem **290**:27460-27472. doi:M115.683706 [pii];10.1074/jbc.M115.683706 [doi].

17. **Di, M., I, C. Lamperti, and V. Tiranti**. 2015. Mitochondrial diseases caused by toxic compound accumulation: from etiopathology to therapeutic approaches. EMBO Mol.Med. **7**:1257-1266. doi:emmm.201505040 [pii];10.15252/emmm.201505040 [doi].

18. **Dowler, S., L. Montalvo, D. Cantrell, N. Morrice, and D. R. Alessi**. 2000. Phosphoinositide 3-kinase-dependent phosphorylation of the dual adaptor for phosphotyrosine and 3-phosphoinositides by the Src family of tyrosine kinase. Biochem.J. **349**:605-610.

19. **Eickholt, B. J., G. Towers, W. J. Ryves, D. Eikel, K. Adley, L. Ylinen, N. Chadborn, A. Harwood, H. Nau, and R. S. Williams**. 2005. Effects of valproic acid derivatives on inositol trisphosphate depletion, teratogenicity, GSK-3b inhibition and viral replication - A screening approach for new bipolar disorder drugs based on the valproic acid core structure. Mol.Pharmacol. **67**:1-8.

20. **Emdal, K. B., A. K. Pedersen, D. B. Bekker-Jensen, K. P. Tsafou, H. Horn, S. Lindner, J. H. Schulte, A. Eggert, L. J. Jensen, C. Francavilla, and J. V. Olsen**. 2015. Temporal proteomics of NGF-TrkA signaling identifies an inhibitory role for the E3 ligase Cbl-b in neuroblastoma cell differentiation. Sci.Signal. **8**:ra40. doi:8/374/ra40 [pii];10.1126/scisignal.2005769 [doi].

21. **Faix, J., L. Kreppel, G. Shaulsky, M. Schleicher, and A. R. Kimmel**. 2004. A rapid and efficient method to generate multiple gene disruptions in *Dictyostelium discoideum* using a single selectable marker and the Cre-loxP system. Nucleic Acids Res. **32**:e143.

22. **Fets, L., J. M. Nichols, and R. R. Kay**. 2014. A PIP5 kinase essential for efficient chemotactic signaling. Curr.Biol. **24**:415-421. doi:S0960-9822(13)01611-4 [pii];10.1016/j.cub.2013.12.052 [doi].

23. **Fey, P., R. J. Dodson, S. Basu, and R. L. Chisholm**. 2013. One stop shop for everything Dictyostelium: dictyBase and the Dicty Stock Center in 2012. Methods Mol.Biol. **983**:59-92. doi:10.1007/978-1-62703-302-2_4 [doi].

24. **Fischbach, A., S. Adelt, A. Muller, and G. Vogel**. 2006. Disruption of inositol biosynthesis through targeted mutagenesis in Dictyostelium discoideum: generation and characterization of inositol-auxotrophic mutants. Biochem.J. **397**:509-518. doi:BJ20060277 [pii];10.1042/BJ20060277 [doi].

25. **Francione, L. M. and P. R. Fisher**. 2011. Heteroplasmic mitochondrial disease in Dictyostelium discoideum. Biochem.Pharmacol. **82**:1510-1520. doi:S0006-2952(11)00529-6 [pii];10.1016/j.bcp.2011.07.071 [doi].

26. **Gelber, D., J. Levine, and R. H. Belmaker**. 2001. Effect of inositol on bulimia nervosa and binge eating. Int.J.Eat.Disord. **29**:345-348. doi:10.1002/eat.1028 [pii].

27. **Hoeller, O. and R. R. Kay**. 2007. Chemotaxis in the absence of PIP3 gradients. Curr.Biol. **17**:813-817.

28. **Ju, S. and M. L. Greenberg**. 2003. Valproate disrupts regulation of inositol responsive genes and alters regulation of phospholipid biosynthesis. Mol.Microbiol. **49**:1595-1603.

29. **Junemann, A., M. Winterhoff, B. Nordholz, K. Rottner, L. Eichinger, R. Graf, and J. Faix**. 2013. ForC lacks canonical formin activity but bundles actin filaments and is required for multicellular development of Dictyostelium cells. Eur.J.Cell Biol. **92**:201-212. doi:S0171-9335(13)00046-0 [pii];10.1016/j.ejcb.2013.07.001 [doi].

30. **Kennington, A. S., C. R. Hill, J. Craig, C. Bogardus, I. Raz, H. K. Ortmeyer, B. C. Hansen, G. Romero, and J. Larner**. 1990. Low urinary chiro-inositol excretion in non-insulin-dependent diabetes mellitus. N.Engl.J.Med. **323**:373-378. doi:10.1056/NEJM199008093230603 [doi].

31. **Kim, K. H. and M. S. Lee**. 2014. Autophagy--a key player in cellular and body metabolism. Nat.Rev.Endocrinol. **10**:322-337. doi:nrendo.2014.35 [pii];10.1038/nrendo.2014.35 [doi].

32. **Klopfenstein, D. R., M. Tomishige, N. Stuurman, and R. D. Vale**. 2002. Role of phosphatidylinositol(4,5)bisphosphate organization in membrane transport by the Unc104 kinesin motor. Cell **109**:347-358. doi:S0092867402007080 [pii].

33. **Kofman, O., W. R. Sherman, V. Katz, and R. H. Belmaker**. 1993. Restoration of brain myo-inositol levels in rats increases latency to lithium-pilocarpine seizures. Psychopharmacology (Berl) **110**:229-234.

34. **Kosta, A., C. Roisin-Bouffay, M. F. Luciani, G. P. Otto, R. H. Kessin, and P. Golstein**. 2004. Autophagy gene disruption reveals a non-vacuolar cell death pathway in Dictyostelium. J.Biol.Chem **279**:48404-48409. doi:10.1074/jbc.M408924200 [doi];M408924200 [pii].

35. **Kumar, R., S. Rafia, and S. Saran**. 2014. Cloning, expression and characterization of the ornithine decarboxylase gene from Dictyostelium discoideum. Int.J.Dev.Biol. **58**:669-676. doi:140174ss [pii];10.1387/ijdb.140174ss [doi].

36. **Lionaki, E., M. Markaki, K. Palikaras, and N. Tavernarakis**. 2015. Mitochondria, autophagy and age-associated neurodegenerative diseases: New insights into a complex interplay. Biochim.Biophys.Acta **1847**:1412-1423. doi:S0005-2728(15)00068-7 [pii];10.1016/j.bbabio.2015.04.010 [doi].

37. **Logan, M. R. and C. A. Mandato**. 2006. Regulation of the actin cytoskeleton by PIP2 in cytokinesis. Biol.Cell **98**:377-388. doi:BC20050081 [pii];10.1042/BC20050081 [doi].

38. **Ludtmann, M. H., G. P. Otto, C. Schilde, Z. H. Chen, C. Y. Allan, S. Brace, P. W. Beesley, A. R. Kimmel, P. Fisher, R. Killick, and R. S. Williams**. 2014. An ancestral non-proteolytic role for presenilin proteins in multicellular development of the social amoeba Dictyostelium discoideum. J.Cell Sci. **127**:1576-1584. doi:jcs.140939 [pii];10.1242/jcs.140939 [doi].

39. **Maeba, R., H. Hara, H. Ishikawa, S. Hayashi, N. Yoshimura, J. Kusano, Y. Takeoka, D. Yasuda, T. Okazaki, M. Kinoshita, and T. Teramoto**. 2008. Myo-inositol treatment increases serum plasmalogens and decreases small dense LDL, particularly in hyperlipidemic subjects with metabolic syndrome. J.Nutr.Sci.Vitaminol.(Tokyo) **54**:196-202. doi:JST.JSTAGE/jnsv/54.196 [pii].

40. **Majumder, A. L., A. Chatterjee, D. K. Ghosh, and M. Majee**. 2003. Diversification and evolution of L-myo-inositol 1-phosphate synthase. FEBS Lett. **553**:3-10. doi:S0014579303009748 [pii].

41. **McLaurin, J., T. Franklin, A. Chakrabartty, and P. E. Fraser**. 1998. Phosphatidylinositol and inositol involvement in Alzheimer amyloid-beta fibril growth and arrest. J.Mol.Biol. **278**:183-194. doi:S0022-2836(98)91677-1 [pii];10.1006/jmbi.1998.1677 [doi].

42. **Michell, R. H., V. L. Heath, M. A. Lemmon, and S. K. Dove**. 2006. Phosphatidylinositol 3,5-bisphosphate: metabolism and cellular functions. Trends Biochem.Sci. **31**:52-63. doi:S0968-0004(05)00343-9 [pii];10.1016/j.tibs.2005.11.013 [doi].

43. **Motoi, Y., K. Shimada, K. Ishiguro, and N. Hattori**. 2014. Lithium and autophagy. ACS Chem Neurosci. **5**:434-442. doi:10.1021/cn500056q [doi].

44. **Mueller, B., E. J. Klemm, E. Spooner, J. H. Claessen, and H. L. Ploegh**. 2008. SEL1L nucleates a protein complex required for dislocation of misfolded glycoproteins. Proc.Natl.Acad.Sci.U.S.A **105**:12325-12330. doi:0805371105 [pii];10.1073/pnas.0805371105 [doi].

45. **Ohnishi, T., T. Murata, A. Watanabe, A. Hida, H. Ohba, Y. Iwayama, K. Mishima, Y. Gondo, and T. Yoshikawa**. 2014. Defective craniofacial development and brain function in a mouse model for depletion of intracellular inositol synthesis. J.Biol.Chem **289**:10785-10796. doi:M113.536706 [pii];10.1074/jbc.M113.536706 [doi].

46. **Otto, G. P., M. Y. Wu, N. Kazgan, O. R. Anderson, and R. H. Kessin**. 2003. Macroautophagy is required for multicellular development of the social amoeba Dictyostelium discoideum. J.Biol.Chem **278**:17636-17645. doi:10.1074/jbc.M212467200 [doi];M212467200 [pii].

47. **Pakes, N. K., D. M. Veltman, F. Rivero, J. Nasir, R. Insall, and R. S. Williams**. 2012. The Rac GEF ZizB regulates development, cell motility and cytokinesis in Dictyostelium. J.Cell Sci. **125**:2457-2465. doi:jcs.100966 [pii];10.1242/jcs.100966 [doi].

48. **Palatnik, A., K. Frolov, M. Fux, and J. Benjamin**. 2001. Double-blind, controlled, crossover trial of inositol versus fluvoxamine for the treatment of panic disorder. J.Clin.Psychopharmacol. **21**:335-339.

49. **Robery, S., J. Mukanowa, S. N. Percie du, P. L. Andrews, and R. S. Williams**. 2011. Investigating the effect of emetic compounds on chemotaxis in Dictyostelium identifies a non-sentient model for bitter and hot tastant research. PLoS.One. **6**:e24439. doi:10.1371/journal.pone.0024439 [doi];PONE-D-11-04761 [pii].

50. **Robery, S., R. Tyson, C. Dinh, A. Kuspa, A. A. Noegel, T. Bretschneider, P. L. Andrews, and R. S. Williams**. 2013. A novel human receptor involved in bitter tastant detection identified using Dictyostelium discoideum. J.Cell Sci. **126**:5465-5476. doi:jcs.136440 [pii];10.1242/jcs.136440 [doi].

51. **Schiebler, M., K. Brown, K. Hegyi, S. M. Newton, M. Renna, L. Hepburn, C. Klapholz, S. Coulter, A. Obregon-Henao, T. M. Henao, R. Basaraba, B. Kampmann, K. M. Henry, J. Burgon, S. A. Renshaw, A. Fleming, R. R. Kay, K. E. Anderson, P. T. Hawkins, D. J. Ordway, D. C. Rubinsztein, and R. A. Floto**. 2015. Functional drug screening reveals anticonvulsants as enhancers of mTOR-independent autophagic killing of Mycobacterium tuberculosis through inositol depletion. EMBO Mol.Med. **7**:127-139. doi:emmm.201404137 [pii];10.15252/emmm.201404137 [doi].

52. **Scioscia, M., S. Kunjara, K. Gumaa, P. McLean, C. H. Rodeck, and T. W. Rademacher**. 2007. Urinary excretion of inositol phosphoglycan P-type in gestational diabetes mellitus. Diabet.Med. **24**:1300-1304. doi:DME2267 [pii];10.1111/j.1464-5491.2007.02267.x [doi].

53. **Shaltiel, G., S. Mark, O. Kofman, R. H. Belmaker, and G. Agam**. 2007. Effect of valproate derivatives on human brain myo-inositol-1-phosphate (MIP) synthase activity and amphetamine-induced rearing. Pharmacol.Rep. **59**:402-407.

54. **Shamir, A., G. Shaltiel, M. L. Greenberg, R. H. Belmaker, and G. Agam**. 2003. The effect of lithium on expression of genes for inositol biosynthetic enzymes in mouse hippocampus; a comparison with the yeast model. Brain Res.Mol.Brain Res. **115**:104-110.

55. **Shetty, A., A. Swaminathan, and J. M. Lopes**. 2013. Transcription regulation of a yeast gene from a downstream location. J.Mol.Biol. **425**:457-465. doi:S0022-2836(12)00890-X [pii];10.1016/j.jmb.2012.11.018 [doi].

56. **Shi, Y., D. L. Vaden, S. Ju, D. Ding, J. H. Geiger, and M. L. Greenberg**. 2005. Genetic perturbation of glycolysis results in inhibition of de novo inositol biosynthesis. J.Biol.Chem **280**:41805-41810. doi:M505181200 [pii];10.1074/jbc.M505181200 [doi].

57. **Shimohama, S., H. Tanino, Y. Sumida, J. Tsuda, and S. Fujimoto**. 1998. Alteration of myo-inositol monophosphatase in Alzheimer's disease brains. Neurosci.Lett. **245**:159-162. doi:S0304394098002092 [pii].

58. **Shimon, H., G. Agam, R. H. Belmaker, T. M. Hyde, and J. E. Kleinman**. 1997. Reduced frontal cortex inositol levels in postmortem brain of suicide victims and patients with bipolar disorder. Am.J.Psychiatry **154**:1148-1150. doi:10.1176/ajp.154.8.1148 [doi].

59. **Shimon, H., Y. Sobolev, M. Davidson, V. Haroutunian, R. H. Belmaker, and G. Agam**. 1998. Inositol levels are decreased in postmortem brain of schizophrenic patients. Biol.Psychiatry **44**:428-432. doi:S0006-3223(98)00071-7 [pii].

60. **Shimshoni, J. A., E. C. Dalton, A. Jenkins, S. Eyal, K. Kwan, R. S. Williams, N. Pessah, B. Yagen, A. J. Harwood, and M. Bialer**. 2007. The effects of CNS-active Valproic acid constitutional isomers, cyclopropyl analogues and amide derivatives on neuronal growth cone behaviour. Mol.Pharmacol. **71**:884-892.

61. **Silverstone, P. H., B. M. McGrath, and H. Kim**. 2005. Bipolar disorder and myo-inositol: a review of the magnetic resonance spectroscopy findings. Bipolar.Disord. **7**:1-10. doi:BDI174 [pii];10.1111/j.1399-5618.2004.00174.x [doi].

62. **Steger, D. J., E. S. Haswell, A. L. Miller, S. R. Wente, and E. K. O'Shea**. 2003. Regulation of chromatin remodeling by inositol polyphosphates. Science **299**:114-116. doi:10.1126/science.1078062 [doi];1078062 [pii].

63. **Szappanos, B., K. Kovacs, B. Szamecz, F. Honti, M. Costanzo, A. Baryshnikova, G. Gelius-Dietrich, M. J. Lercher, M. Jelasity, C. L. Myers, B. J. Andrews, C. Boone, S. G. Oliver, C. Pal, and B. Papp**. 2011. An integrated approach to characterize genetic interaction networks in yeast metabolism. Nat.Genet. **43**:656-662. doi:ng.846 [pii];10.1038/ng.846 [doi].

64. **Tarassov, K., V. Messier, C. R. Landry, S. Radinovic, M. M. Serna Molina, I. Shames, Y. Malitskaya, J. Vogel, H. Bussey, and S. W. Michnick**. 2008. An in vivo map of the yeast protein interactome. Science **320**:1465-1470. doi:1153878 [pii];10.1126/science.1153878 [doi].

65. **Terbach, N. and R. S. Williams**. 2009. Structure-function studies for the panacea, valproic acid. Biochem.Soc.Trans **37**:1126-1132.

66. **Tikhonenko, I., V. Magidson, R. Graf, A. Khodjakov, and M. P. Koonce**. 2013. A kinesin-mediated mechanism that couples centrosomes to nuclei. Cell Mol.Life Sci. **70**:1285-1296. doi:10.1007/s00018-012-1205-0 [doi].

67. **Toker, L., Y. Bersudsky, I. Plaschkes, V. Chalifa-Caspi, G. T. Berry, R. Buccafusca, D. Moechars, R. H. Belmaker, and G. Agam**. 2014. Inositol-related gene knockouts mimic lithium's effect on mitochondrial function. Neuropsychopharmacology **39**:319-328. doi:npp2013194 [pii];10.1038/npp.2013.194 [doi].

68. **Trushina, E., E. Nemutlu, S. Zhang, T. Christensen, J. Camp, J. Mesa, A. Siddiqui, Y. Tamura, H. Sesaki, T. M. Wengenack, P. P. Dzeja, and J. F. Poduslo**. 2012. Defects in mitochondrial dynamics and metabolomic signatures of evolving energetic stress in mouse models of familial Alzheimer's disease. PLoS.One. **7**:e32737. doi:10.1371/journal.pone.0032737 [doi];PONE-D-11-21642 [pii].

69. **Vaden, D. L., D. Ding, B. Peterson, and M. L. Greenberg**. 2001. Lithium and valproate decrease inositol mass and increase expression of the yeast INO1 and INO2 genes for inositol biosynthesis. J.Biol.Chem. **276**:15466-15471.

70. **Van Lookeren Campagne, M. M., C. Erneux, E. R. Van, and P. J. Van Haastert**. 1988. Two dephosphorylation pathways of inositol 1,4,5-trisphosphate in homogenates of the cellular slime mould Dictyostelium discoideum. Biochem.J. **254**:343-350.

71. **Waheed, A., M. H. Ludtmann, N. Pakes, S. Robery, A. Kuspa, C. Dinh, D. Baines, R. S. Williams, and M. A. Carew**. 2014. Naringenin inhibits the growth of Dictyostelium and MDCK-

derived cysts in a TRPP2 (polycystin-2)-dependent manner. Br.J.Pharmacol. **171**:2659-2670. doi:10.1111/bph.12443 [doi].

72. **Wang, H. and D. P. Raleigh**. 2014. General amyloid inhibitors? A critical examination of the inhibition of IAPP amyloid formation by inositol stereoisomers. PLoS.One. **9**:e104023. doi:10.1371/journal.pone.0104023 [doi];PONE-D-14-14660 [pii].

73. **Wessels, D., D. F. Lusche, A. Scherer, S. Kuhl, M. A. Myre, and D. R. Soll**. 2014. Huntingtin regulates Ca(2+) chemotaxis and K(+)-facilitated cAMP chemotaxis, in conjunction with the monovalent cation/H(+) exchanger Nhe1, in a model developmental system: insights into its possible role in Huntingtons disease. Dev.Biol. **394**:24-38. doi:S0012-1606(14)00400-X [pii];10.1016/j.ydbio.2014.08.009 [doi].

74. **Williams, R. S. B., L. Cheng, A. W. Mudge, and A. J. Harwood**. 2002. A common mechanism of action for three mood-stabilizing drugs. Nature **417**:292-295.

75. **Williams, R. S. B., W. J. Ryves, E. C. Dalton, B. Eickholt, G. Shaltiel, G. Agam, and A. J. Harwood**. 2005. A molecular cell biology of lithium. Biochem.Soc.Trans. **32**:799-802.

FIGURE 1. Inositol Signalling, and the Conservation of the Ino1 Protein in *Dictyostelium* and Humans. (A) Inositol metabolism. Ino1 converts glucose 6-phosphate to inositol-3-phosphate, which is a rate-limiting step in inositol production. (B) Sequence homology between the human (Q9NPH2-1) and *Dictyostelium* (Q54N49) Ino1 is present throughout the proteins. Identical amino acids are shown in dark blue. The NAD binding and catalytic domains are among the four regions that are highly conserved in eukaryotic Ino1 proteins: GWGGNNG (yellow), LWTANTERY (blue), SYNHLGNNDG (green) and NGSPQNTFVPGL (purple). The tetramerisation domain containing a putative catalytic site (with the conserved amino acid residues SYNHLGNNDG) is shown in red. The amino acids that were ablated in *Dictyostelium* Ino1 are shown by the horizontal black line. (C) Alignment of the conserved regions of Ino1 proteins from various species, where '*' denotes identity, ':' high conservation, '.' low conservation levels. (D) Schematic representation of the strategy used to prepare the *ino1* knock-out construct. N- and C-terminal portions of the *ino1* gene were cloned into knock-out vector flanking blasticidin resistance (*bsr*) gene and the knock-out cassette was transformed into *Dictyostelium* cells, where homologous recombination deleted a portion of the *ino1* gene and disrupts the open reading frame. (E) PCR screening strategy to identify *ino1*$^{-}$ mutants, showing primers locations for genomic and vector controls, the diagnostic knock-out product, and spanning the inserted *bsr* gene present in the *ino1*$^{-}$ knock-out. (F) PCR results showing the ablation of part of the *ino1* gene in the *ino1*$^{-}$ mutant, in comparison to wild-type cells. INO1 - inositol 3-phosphate synthase; IMPase - inositol monophosphatase; IPPase - inositol polyphosphate 1-phosphatase; IP2 - inositol bisphosphate; IP3 - inositol trisphosphate; PLC - phospholipase C; PI – phosphatidylinositol; PIP - phosphatidylinositol phosphate; PIP2 - phosphatidylinositol bisphosphate; PIP3 - phosphatidylinositol trisphosphate.

FIGURE 2. Ablating *ino1* in *Dictyostelium* Causes Inositol Auxotrophy. (A) *Dictyostelium* cells grown in liquid medium show rapid growth up to a stationary phase (at 168h). Ablation of *ino1* blocks cell growth in the absence of exogenous inositol, with only partial restoration of wild-type growth by the addition of either 300 μM or 500 μM inositol. (B) During starvation, wild-type *Dictyostelium* forms fruiting bodies without inositol pre-treatment. Under the same conditions, *ino1*$^-$ cells are unable to form fruiting bodies. Fruiting body formation in *ino1*$^-$ cells is restored when the cells are grown with inositol supplementation prior to the assay. (C) Expressing *ino1-RFP* in *Dictyostelium ino1*$^-$ cells was confirmed by reverse transcription PCR (RTPCR); with an Ig7 gene control, and Western blot analysis to show the full length protein (with a ladder in kDa), that (D) restores growth rate and (E) is present in the cytosol and (F) restores development in the absence of exogenous inositol. (G) *ino1*$^-$ cells are unable to grow on agar plates seeded with bacteria, and expressing *ino1-RFP* in these cells restores bacterial growth. Error bars represent SEM. Statistical significance was determined by an unpaired two-tailed *t*-test, ***$p < 0.001$; n = 3.

FIGURE 3. Inositol Depletion Causes a Change in Velocity and Cell Shape, an Activation of Autophagy, a Loss in Cell-Substrate Adhesion and a Reduction in Cytokinesis in *Dictyostelium ino1*$^-$ Cells. (A) The level of *myo*-inositol analysed by NMR in the wild-type and *ino1*$^-$ cells grown with (500 μM) or without exogenous inositol for 12 or 24 hours, or following inositol re-introduction. Inositol levels were reduced in the *ino1*$^-$ mutant following inositol depletion for 12 and 24 hours, and restored to basal levels following reintroduction for 12 hours. (B) Average velocity, aspect and persistence of aggregation-competent *ino1*$^-$ cells (grown with 500 μM inositol, or without inositol, for 24 hours prior to imaging) or wild-type cells during chemotaxis towards cAMP. Velocity shows the distance travelled by cells over time. Aspect refers to the roundness of cells (1 = perfectly round). Directness is a ratio of the

distance travelled by a cell compared to the total direct distance, where 1 represents a straight line. (D) Autophagosomes were visualised in wild-type and *ino1*$^{-}$ cells expressing Atg8-GFP and (E) quantified in the presence or absence (24 hours) of inositol treatment. (F) Cell adhesion was monitored in wild-type and *ino1*$^{-}$ cells, and in *ino1*$^{-}$ cells expressing *ino1*-RFP, in the presence (500 µM) and absence of inositol for at least 24 hours. (G) Cytokinesis was examined in wild-type and *ino1*$^{-}$ cells, and in *ino1*$^{-}$ cells expressing *ino1*-RFP, using DAPI nuclear stain to label cell nuclei, and (H) the number of nuclei per cell was quantified. Error bars represent SEM. Statistical significance was determined by (A&B,C,E,F) an unpaired two-tailed *t*-test, (H) 2-way ANOVA with Bonferroni post-test, *$p < 0.05$, ***$p < 0.001$; (C) $n \geq 25$ cells analysed per condition; (E) $n \geq 117$ cells analysed per condition; (F) $n = 3$ repeats; (H) $n \geq 250$ cells analysed per condition.

FIGURE 4. Inositol Depletion Affects Phosphoinositides Levels in *Dictyostelium*. (A) The structure of phosphoinositol showing diacyl or ether/acyl fatty acid linkages to a glycerol backbone and inositol head group. (B) Metabolic pathway depicting phospholipid production from phosphatidic acid (PA) as an example. (C-Q) To monitor phospholipids in wild-type and the *ino1*$^{-}$ mutant, cells were grown in the presence of inositol (500 µM, denoted '+'), the absence of inositol (12 or 24h; denoted '+/-') or with inositol added after a 24h depletion period (500 µM for 12h; denoted '+/-/+') and control denotes without inositol supplementation. The levels of ether/acyl (C34:1ea) or diacyl (C36:3aa) phospholipids are shown as a percentage relative to phospholipid levels present in the wild-type strain grown in the absence of inositol. Inositol depletion reduced the levels of diacyl PI, PIP and PIP2 phosphoinositides; the level of PIP3 was undetectable, and reduced the levels of ether/acyl PIP and PIP3. Error bars represent SEM. Statistical analysis was carried out between wild-type (+ inositol) and *ino1*$^{-}$ (+ inositol)

by unpaired two-tailed *t*-test to illustrate the significance of changes due to the loss of the Ino1 protein, shown as "*", *p < 0.05, **p < 0.01, ***p < 0.001.

FIGURE 5. Comparison of Metabolic Profiles of *Dictyostelium* Following Ino1 Loss and Inositol Depletion. To monitor metabolic profiles in the wild-type and the *ino1*$^{-}$ mutant, cells were grown in the presence of inositol (500 μM, denoted '+'), the absence of inositol (12 or 24h; denoted '+/-') or in inositol added after 24h depletion period (500 μM for 12h; denoted '+/-/+'), and control denotes without inositol supplementation. (A) Metabolic variations existing between cell type and *myo*-inositol exposure were assessed by principal component analysis (PCA) generated from the ^{1}H-NMR spectra of the *Dictyostelium* metabolic fingerprints. The main source of variation (53%) was driven by the mutation while inositol depletion accounted for approximately 12% of the metabolic variation in this dataset. (B) Loadings plot associated with PC1 (red peaks pointing upwards are positively associated with PC1 while those pointing downwards are negatively associated with PC1). (C) Loadings plot associated with PC2.

FIGURE 6. Metabolic profile analysis of the *ino1*$^{-}$ mutant. Cells were grown in the presence of inositol (500 μM, denoted '+'), the absence of inositol (12 or 24h; denoted '+/-') or in inositol added after 24h depletion period (500 μM for 12h; denoted '+/-/+'). (A,B) Metabolic changes induced by *ino1* ablation. Orthogonal projection to latent structure discriminant analysis (O-PLS DA) was used in order to determine the specific impact of the mutation on cell metabolism. (A) Plot of the scores against the cross-validated scores generated by the O-PLS DA (R^2Y = 0.89, Q2 = 0.88 and *p* value for 500 random permutations = 0.002) using the ^{1}H-NMR spectra of the *Dictyostelium* wild-type and *ino1*$^{-}$ cells (except +/-24/+12h inositol exposure) as a matrix of independent variables and mutation as predictor. (B) Loadings plot of

the O-PLS DA model (peaks in red indicate increased metabolite levels in response to the mutation). (C,D) Effect of inositol treatment on the metabolism of the *ino1*$^{-}$ mutant. (C) Plot of the scores against the cross-validated scores generated by the O-PLS DA ($R^2Y = 0.67$, $Q^2Y = 0.51$ and *p* value for 500 permutations = 0.002) using the ^{1}H-NMR spectra of the *ino1*$^{-}$ cells (-12h and -24h inositol vs + inositol) as a matrix of independent variables and depletion of *myo*-inositol as a predictor. (D) Loadings plot of the O-PLS DA model (peaks in red indicate increased metabolite levels in response to the presence of inositol). (E,F) Reintroduction of *myo*-inositol post deprivation induces a metabolic shift. (E) Plot of the scores against the cross-validated scores generated by the O-PLS DA ($R^2Y= 0.90$, $Q^2Y = 0.86$ and *p* value for 500 permutations = 0.002) using the ^{1}H-NMR spectra of the *ino1*$^{-}$ cells (-12h and -24h inositol vs +/-/+ inositol) as a matrix of independent variables and *myo*-inositol reintroduction as a predictor. (F) Loadings plot of the O-PLS DA model (peaks in red indicate increased metabolite levels in response to the depletion of *myo*-inositol), $n \geq 4$.

FIGURE 7. Levels of metabolites in wild-type and *ino1*$^{-}$ cells grown under varying inositol conditions. Metabolite levels, measured by NMR, were quantified using MATLAB and plotted to illustrate changes observed in wild-type and *ino1*$^{-}$ cells for (A) amino acids (B) cell cycle and DNA-related metabolites (C) other metabolites. Control denotes without inositol supplementation. Error bars represent SEM. Statistical analysis was carried out between wild-type (Ax2) (+ inositol) and *ino1*$^{-}$ (+ inositol) by unpaired two-tailed *t*-test to illustrate the significance of changes due to the loss of Ino1 protein, shown as "*", *$p < 0.05$, **$p < 0.01$, ***$p < 0.001$. A separate unpaired two-tailed *t*-test analysis was used to compare *ino1*$^{-}$ (+ inositol) and *ino1*$^{-}$ (- inositol 12h and 24h), shown as "$^{+}$", $^{+}p < 0.05$, $^{++}p < 0.01$, $^{+++}p < 0.001$.

FIGURE 8. An Ino1 non-catalytic role in *Dictyostelium*. (A) Ino1-RFP protein with an aspartic acid to alanine substitution (*ino1D342A*) in a highly conserved region of a catalytic domain was overexpressed in the wild-type and *ino1*$^-$ cells. In the *ino1*$^-$ cells, the mutated protein was unable to rescue the *ino1*$^-$ inositol auxotrophy, consistent with a catalytically inactive protein. In the wild-type cells, expressing the mutant protein significantly decreased growth, while the addition of exogenous inositol partially rescued this phenotype. Error bars represent SEM for n = 3 repeats. Statistical analysis was carried out for each individual condition compared to wild-type (Ax2) by unpaired two-tailed *t*-test, $*p < 0.05$, $***p < 0.001$. (B) Co-immunoprecipitation of the Ino1-RFP protein (or RFP only control) expressed in *ino1*$^-$ cells, using anti-RFP coated beads, shown for bound (B) and non-bound fractions (NB). SDS-PAGE gels were visualised following Coomassie staining (left) and analysed by Western blot with an anti-RFP antibody (right). Bands specific to Ino1-RFP (and absent from the RFP control) were analysed by mass spectrometry to identify potential Ino1 binding partners. (C) FLAG-tagged potential interacting proteins GpmA, PefB, and Q541X5, were investigated by immunoprecipitation using Ino1-RFP and anti-RFP-coated beads, followed by Western blot analysis with anti-RFP and anti-FLAG antibodies. (D) An Ino1-Q54IX5 interaction was confirmed by immunoprecipitation of the GFP-Q54IX5 protein with anti-GFP-coated beads in the presence of Ino1-RFP (or RFP only) and Western blot analysis with anti-RFP and anti-GFP antibodies.

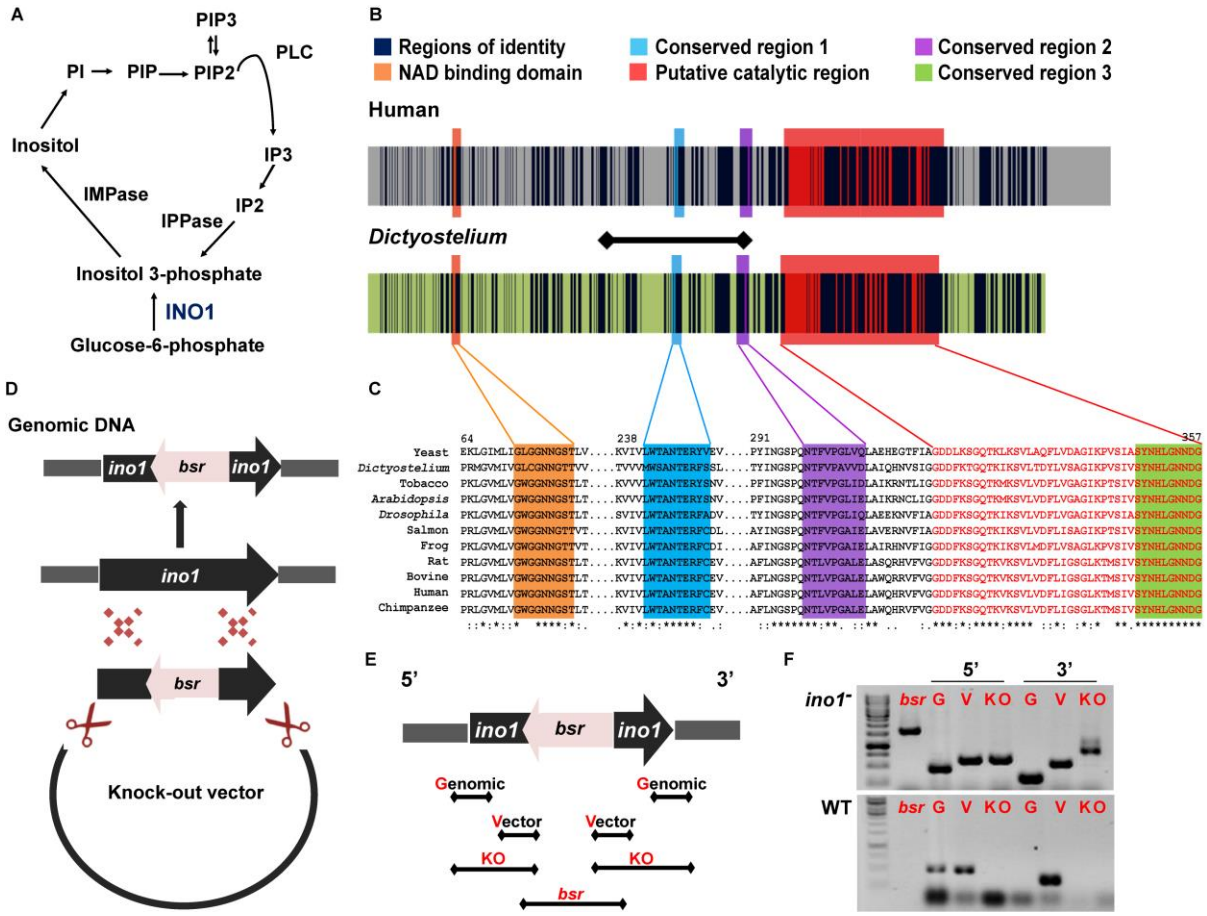
A
PIP3
PLC
PI
PIP
PIP2
Inositol
IP3
IMPase
IPPase
IP2
Inositol 3-phosphate
INO1
Glucose-6-phosphate
B
Regions of identity
Conserved region 1
Conserved region 2
NAD binding domain
Putative catalytic region
Conserved region 3
Human
Dictyostelium
C
64
238
291
357
Yeast
Dictyostelium
Tobacco
Arabidopsis
Drosophila
Salmon
Frog
Rat
Bovine
Human
Chimpanzee
D
Genomic DNA
ino1
bsr
ino1
ino1
bsr
Knock-out vector
E
5'
3'
ino1
bsr
ino1
Genomic
Genomic
Vector
Vector
KO
KO
bsr
F
5'
3'
ino1-
bsr G V KO G V KO
WT
bsr G V KO G V KO

Fig 1

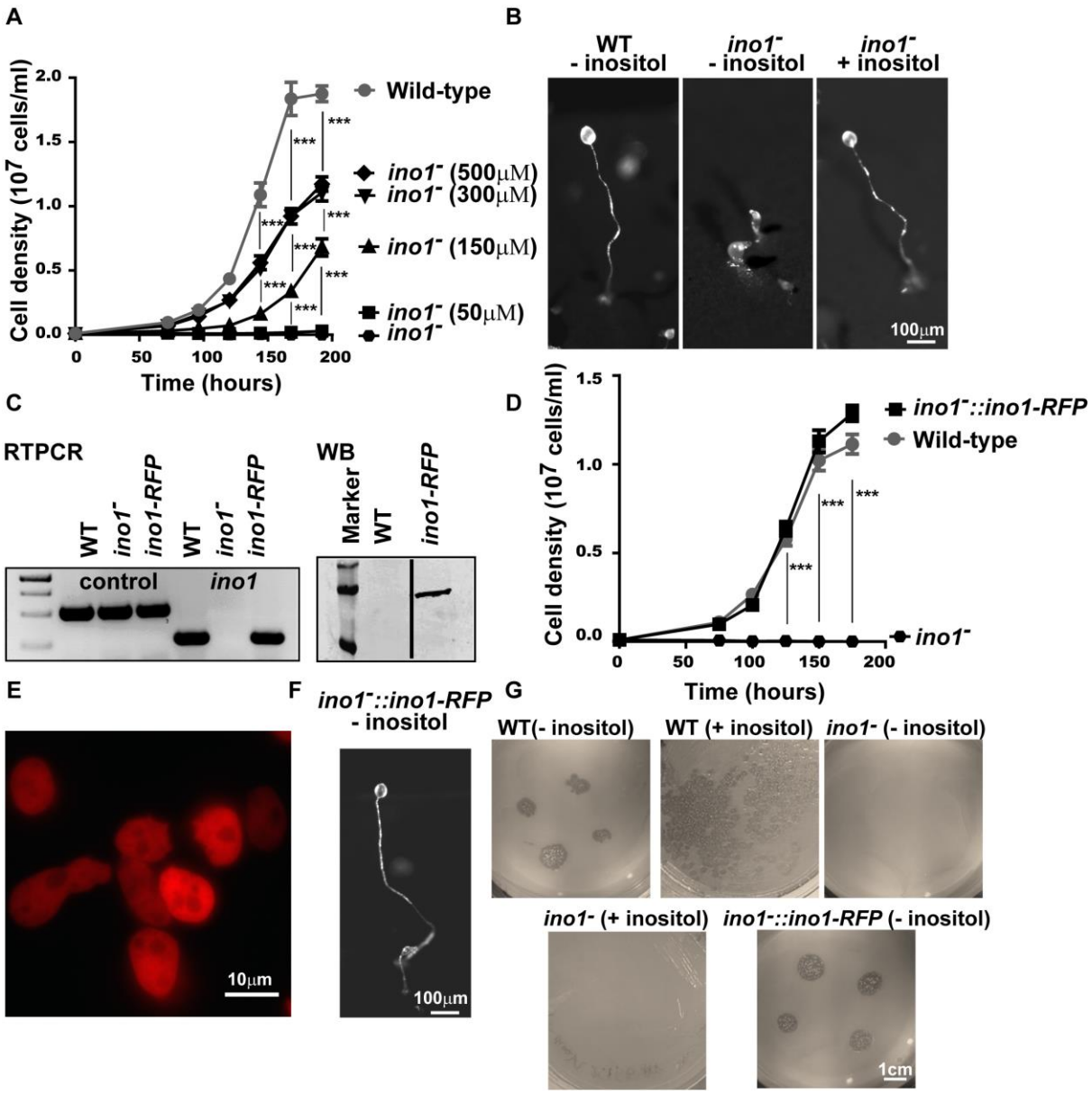
A
Cell density (10^7 cells/ml)
Time (hours)
Wild-type
ino1- (500μM)
ino1- (300μM)
ino1- (150μM)
ino1- (50μM)
ino1-
B
WT - inositol
ino1- - inositol
ino1- + inositol
100μm
C
RTPCR
WT
ino1-
ino1-RFP
control
ino1
WB
Marker
WT
ino1-RFP
D
ino1-::ino1-RFP
Wild-type
ino1-
Cell density (10^7 cells/ml)
Time (hours)
E
10μm
F
ino1-::ino1-RFP - inositol
100μm
G
WT(- inositol)
WT (+ inositol)
ino1- (- inositol)
ino1- (+ inositol)
ino1-::ino1-RFP (- inositol)
1cm

Fig 2

A

Cell Line	Treatment (500 µM inositol)	Concentration (µM) *myo*-inositol
WT (Ax2)	(-)	1.47
	(+)	3.40
	(- 24 h)	1.60
	(+/-12 h /+ 24h)	2.17
ino1⁻	(+)	1.82
	(- 12 h)	0.80
	(- 24 h)	1.15
	(+/-12 h /+ 24h)	1.96

B

Cell Line	Velocity (µm/min)	Aspect	Directness
WT (Ax2)	9.63 ± 1.49	2.96 ±0.61	0.87 ± 0.14
ino1⁻ (+ins)	7.42 ± 3.32	1.63± 0.55***	1.12 ± 0.54
ino1⁻ (-ins)	4.97 ± 1.18 ***	1.76± 0.46***	1.68 ± 0.46*

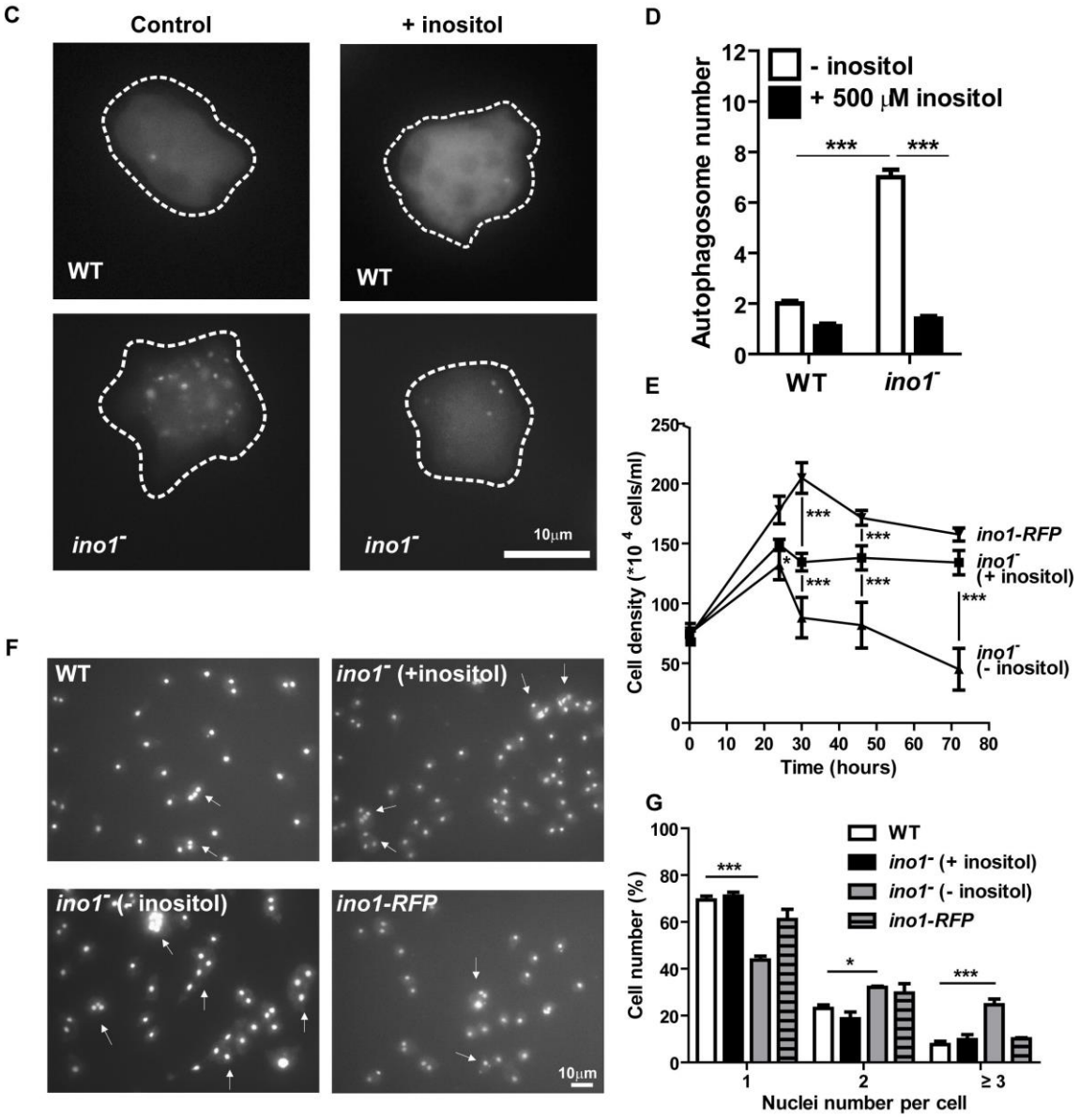

923

924 **Fig 3**

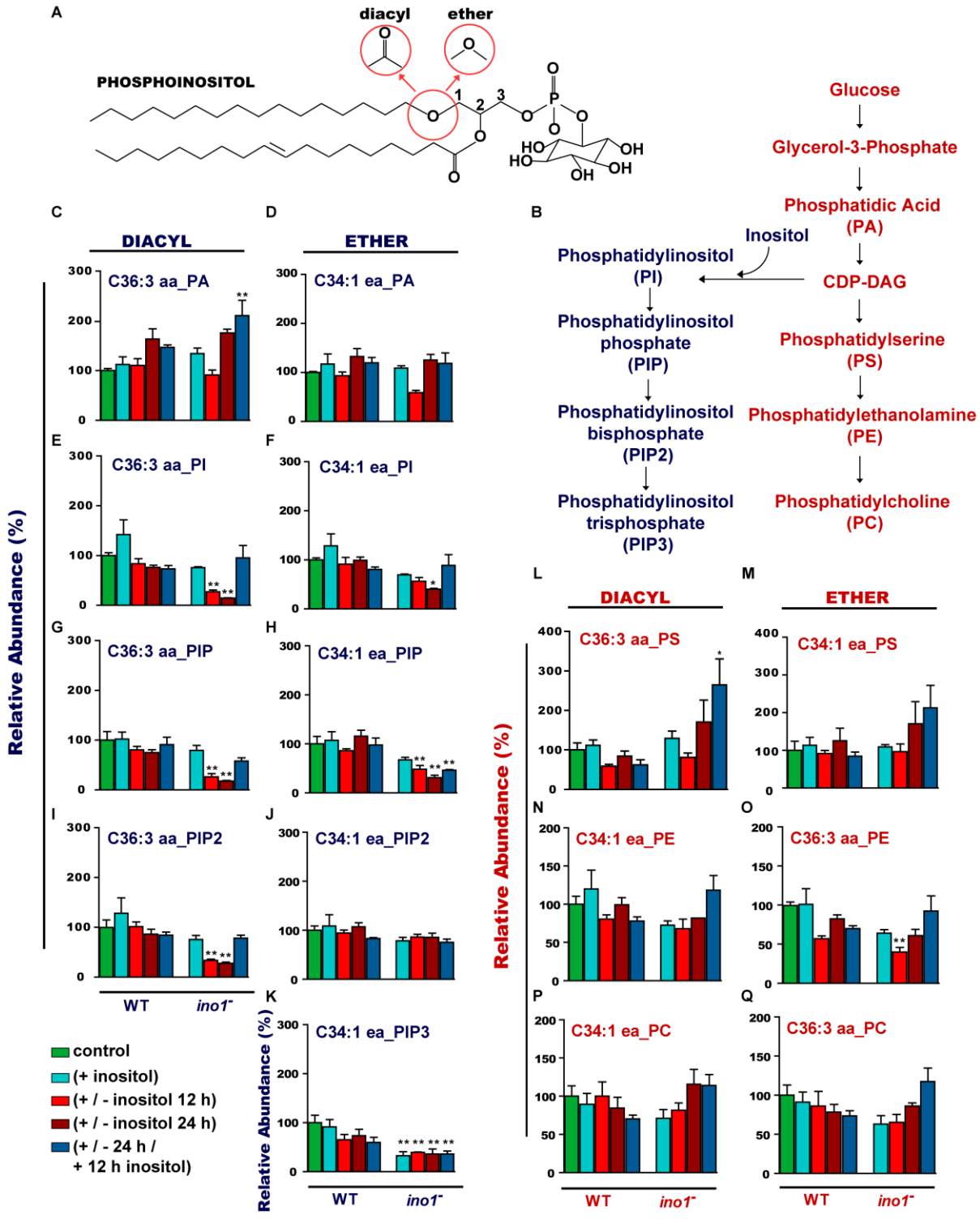
A
diacyl
ether
PHOSPHOINOSITOL
B
Glucose
Glycerol-3-Phosphate
Phosphatidic Acid (PA)
Inositol
Phosphatidylinositol (PI)
CDP-DAG
Phosphatidylinositol phosphate (PIP)
Phosphatidylserine (PS)
Phosphatidylinositol bisphosphate (PIP2)
Phosphatidylethanolamine (PE)
Phosphatidylinositol trisphosphate (PIP3)
Phosphatidylcholine (PC)
C
DIACYL
D
ETHER
C36:3 aa_PA
C34:1 ea_PA
E
C36:3 aa_PI
F
C34:1 ea_PI
G
C36:3 aa_PIP
H
C34:1 ea_PIP
I
C36:3 aa_PIP2
J
C34:1 ea_PIP2
K
C34:1 ea_PIP3
Relative Abundance (%)
WT
ino1-
control
(+ inositol)
(+ / - inositol 12 h)
(+ / - inositol 24 h)
(+ / - 24 h / + 12 h inositol)
L
DIACYL
M
ETHER
C36:3 aa_PS
C34:1 ea_PS
N
C34:1 ea_PE
O
C36:3 aa_PE
P
C34:1 ea_PC
Q
C36:3 aa_PC

Fig 4

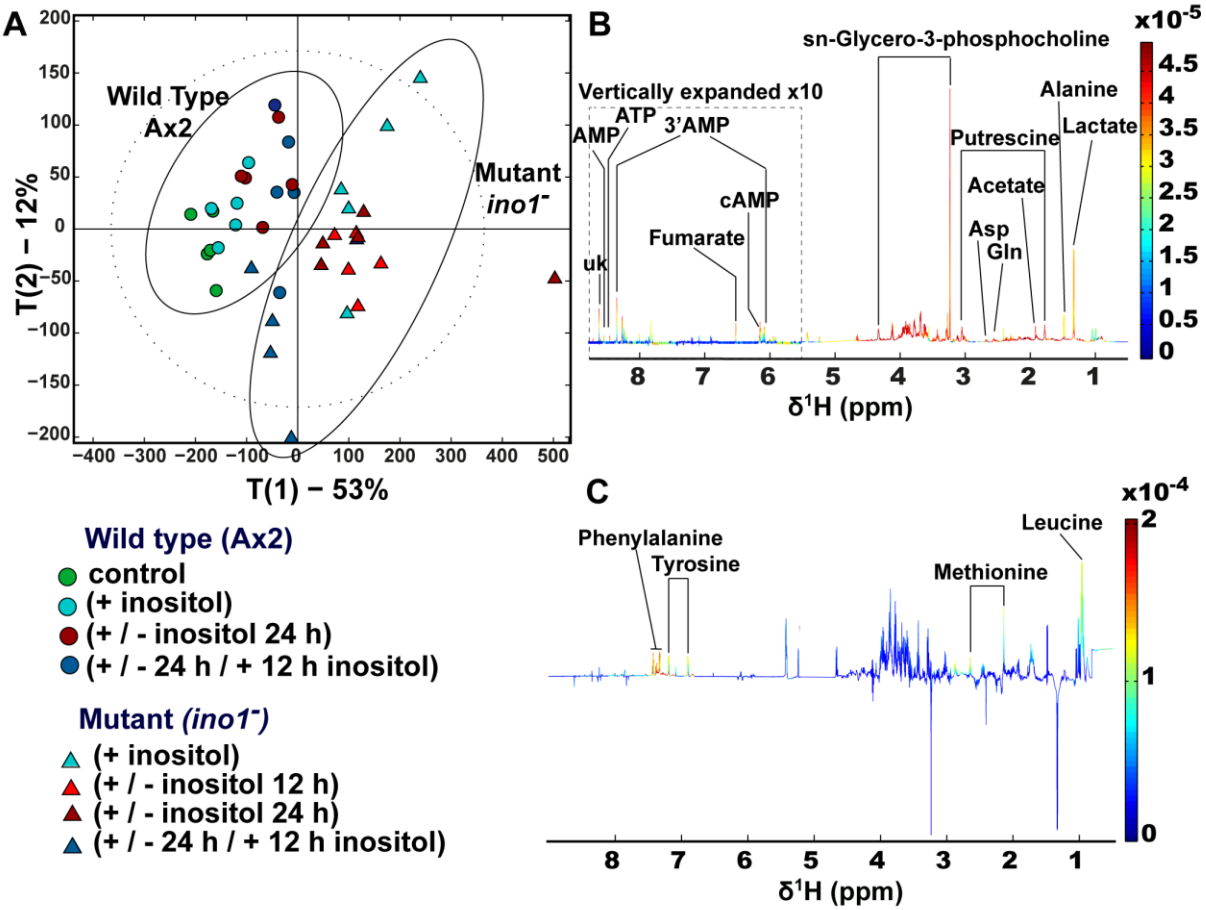

929

930 **Fig 5**

931

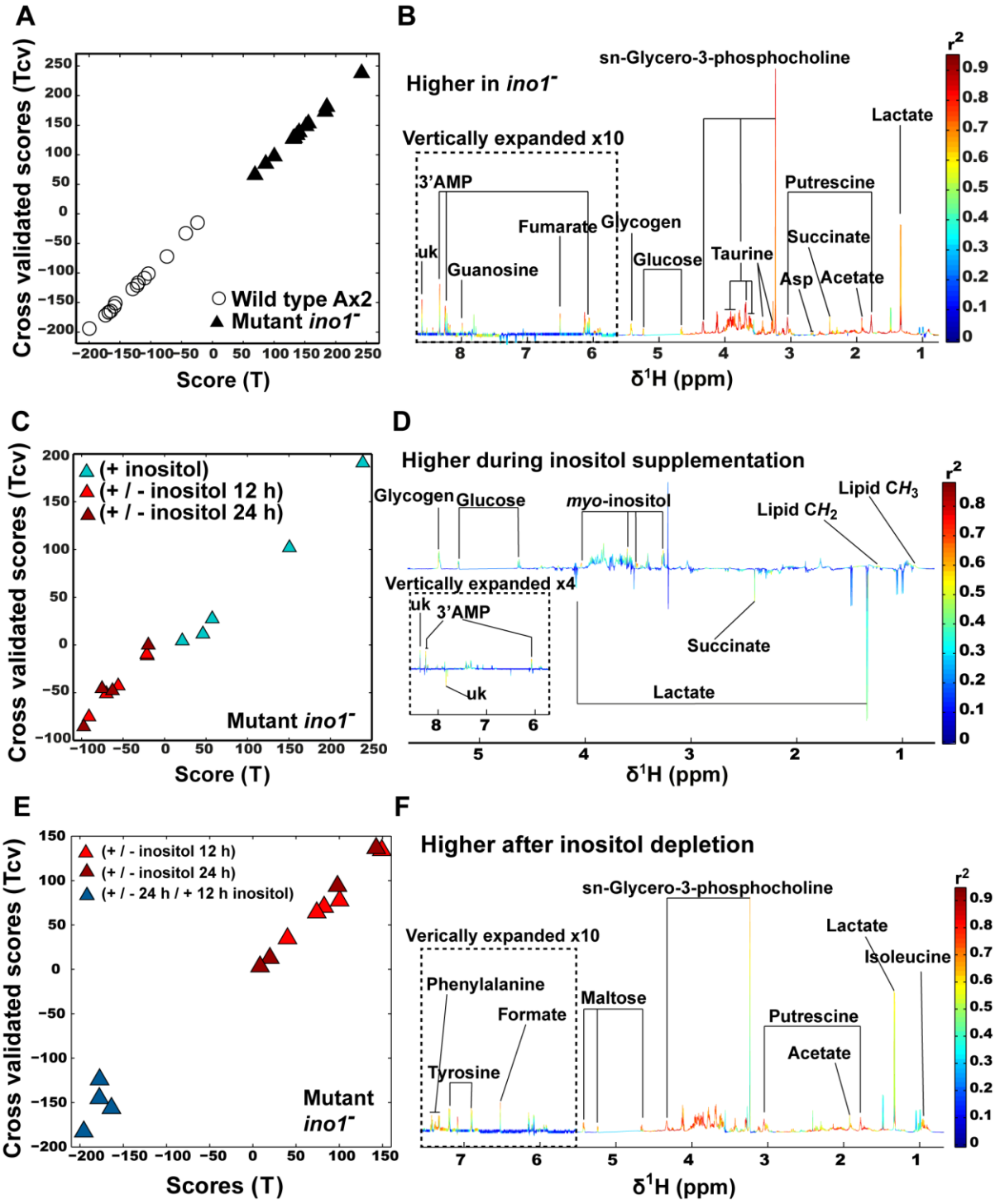

932

933 **Fig 6**

934

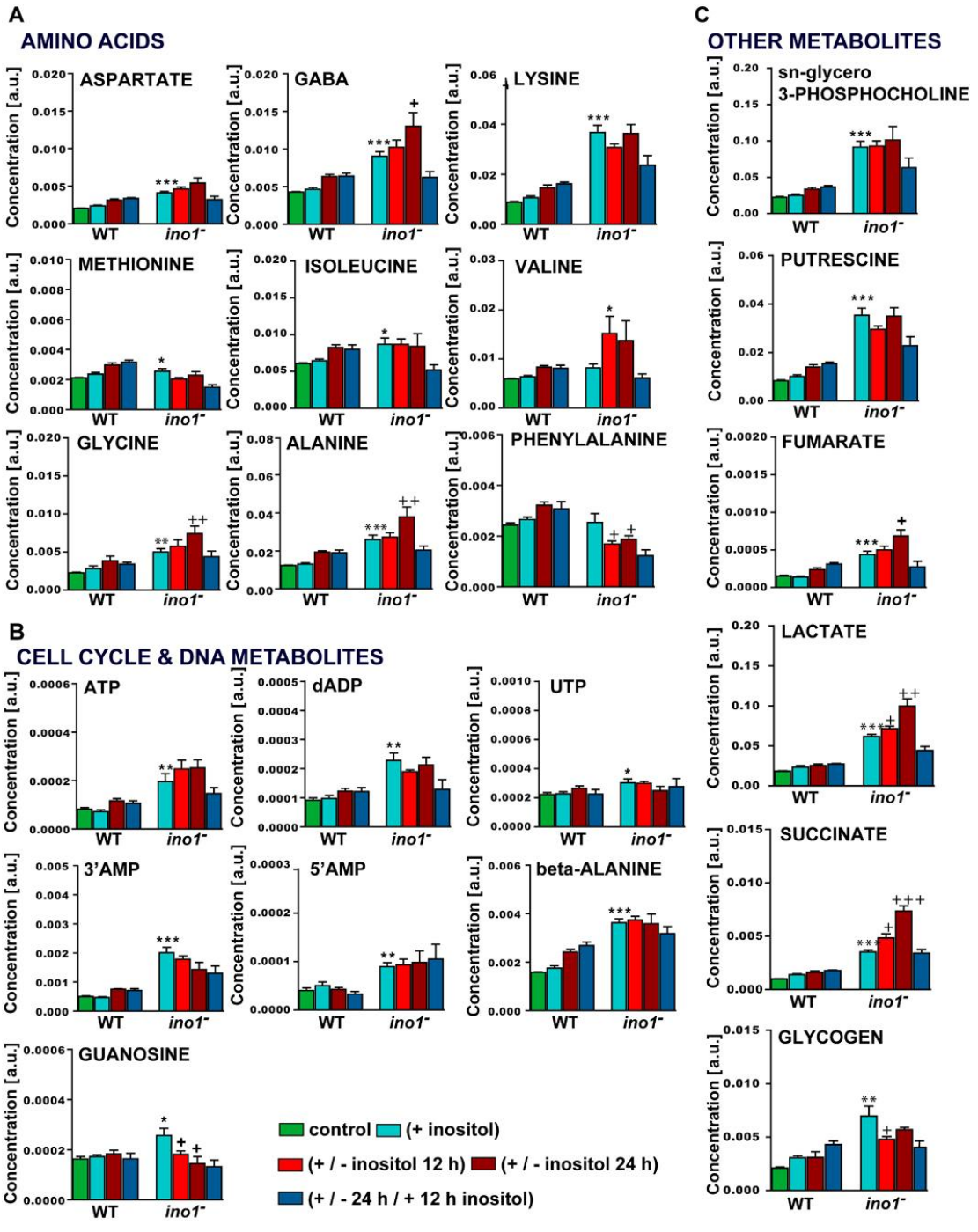
A
AMINO ACIDS
ASPARTATE
GABA
LYSINE
METHIONINE
ISOLEUCINE
VALINE
GLYCINE
ALANINE
PHENYLALANINE
B
CELL CYCLE & DNA METABOLITES
ATP
dADP
UTP
3'AMP
5'AMP
beta-ALANINE
GUANOSINE
C
OTHER METABOLITES
sn-glycero 3-PHOSPHOCHOLINE
PUTRESCINE
FUMARATE
LACTATE
SUCCINATE
GLYCOGEN
Concentration [a.u.]
WT
ino1-
control
(+ inositol)
(+ / - inositol 12 h)
(+ / - inositol 24 h)
(+ / - 24 h / + 12 h inositol)

Fig 7

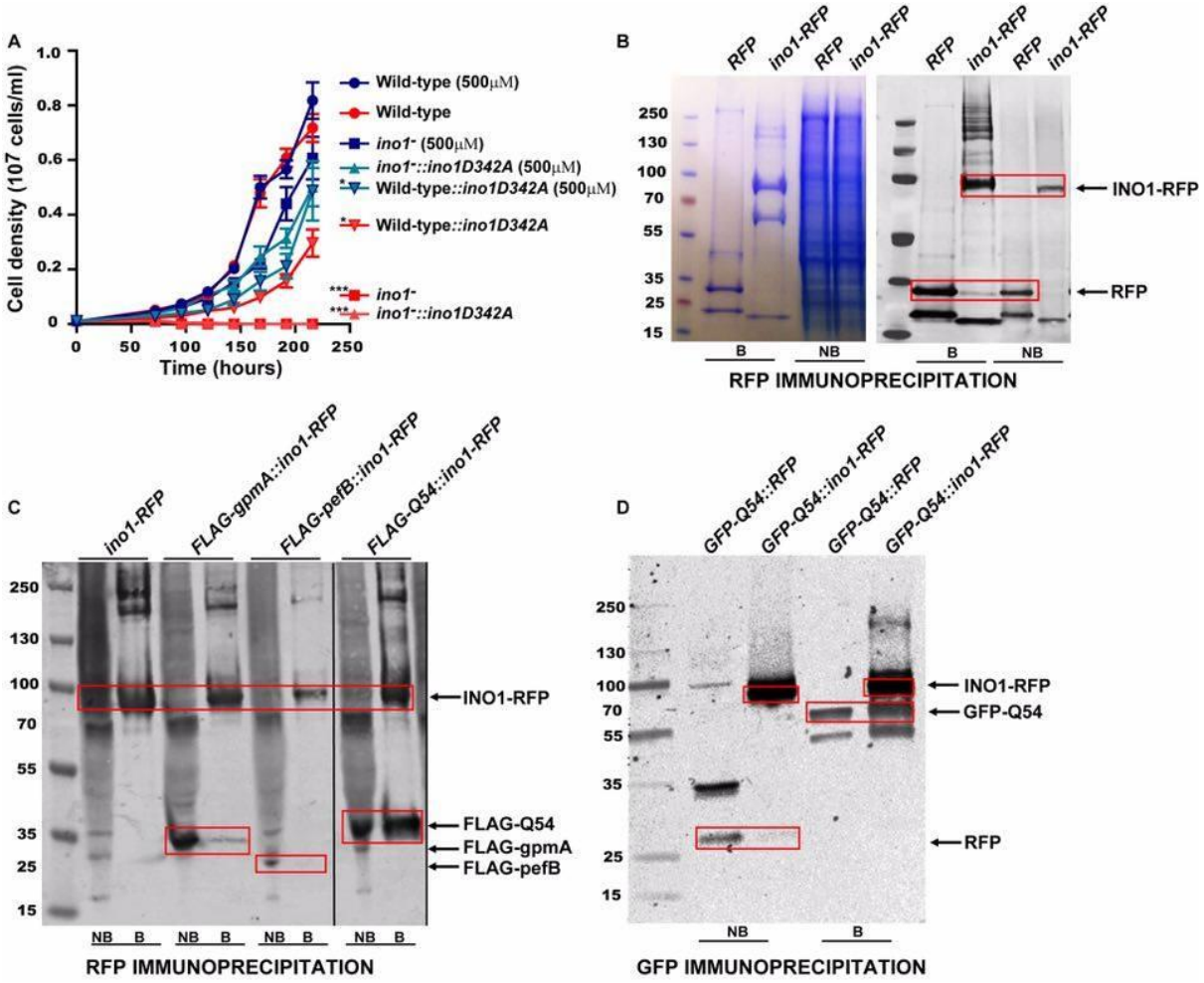

938

939

940 **Fig 8**

941